

Geometric Criteria for Fractional Chern Insulators

Amir Shapour Mohammadi

Senior Thesis
Department of Physics
Princeton University
Fall 2023 - Spring 2024



Adviser: Ali Yazdani
Second reader: F. D. M. Haldane

This paper represents my own work in accordance with University regulations.

/s/ Amir Shapour Mohammadi

Acknowledgements

I would foremost like to praise God - ﷺ. Without His guidance, I would be lost. Without His mercy, I would be nothing.

I am endlessly indebted to my family for the sacrifices they endured that enabled me to be where I am today. I am grateful to God for introducing me to my partner Mahya, who is a source of joy and encouragement.

Thank you to Professor Ali Yazdani for your insights over the past couple of years. Your experimental work and the way you approach problems solidified my passion for this field. Thank you to Professor Duncan Haldane for *countless* hours of his invaluable insight. I am grateful to Professor Jason Petta who provided immense help and direction during my formative years. Thank you also to his group members, and in particular Adam Mills for both professional and personal direction. Thank you to Yen-Chen Tsui, Yuwen Hu, Minhao He, Cheng-Li Chiu, and Ryan Lee of the Yazdani group. Professors Donna Sheng and Biao Lian provided specific, technical assistance for the numerical simulation.

Abstract

Fractional Chern insulators (FCI) realize the physics of the fractional quantum Hall effect (FQHE) in a lattice model and the absence of a magnetic field. The FQHE manifests in Landau levels, topological flat bands with remarkably simple band geometry. Mimicking the band topology alone in the lattice requires intrinsically breaking time-reversal symmetry and guarantees the lattice-analogue of the integer quantum Hall effect known as the Chern insulator, a single-particle effect. The FQHE is a many-body effect which requires flat, topological bands and has been theorized to require so-called ideal band geometry. We will explore the role of band geometry in the manifestation of FCI phases through exact-diagonalization numerical simulations, and discuss recent issues with geometry-dependent criteria.

Contents

1 Electrons in a Lattice	1
1.1 Lattices	1
1.2 Bloch's theorem	2
1.3 Topological argument for studying two dimensions	3
1.4 Tight-binding model	3
2 Integer Quantum Hall Effect	5
2.1 Classical Hall effect	6
2.2 Landau Levels	6
2.3 Hall conductance (naive calculation)	10
2.4 Band geometry	11
2.5 Geometry of Landau levels	14
2.6 Quantized Hall conductivity from topology	15
2.7 Quantized Hall conductivity in Landau levels	17
3 Chern Insulator	18
3.1 Hofstadter bands	19
3.2 Chern insulator models	20
4 Fractional Quantum Hall Effect	22
4.1 Interactions in flat band models	23
4.2 Laughlin states	24
4.3 Haldane pseudopotential	26
4.4 Topological degeneracy of ground state manifold	27
5 Fractional Chern Insulator	28
5.1 Geometric Stability Hypothesis	30
5.2 Geometry-independence	33
6 Numerical Techniques for Simulating Fractional Chern Insulators	37
6.1 Single-band approximation of many-body Hamiltonian	38
6.2 Issues with uniformly choosing gauge	41
6.3 Jordan-Wigner Transformation	43
7 Conclusions	45
References	46

Table 1: Description of most-used variables.

Lattice Hamiltonians	
\mathbf{a}_i	Primitive lattice vectors
$\boldsymbol{\tau}_i$	Nearest-neighbor hopping vectors
α	Sublattice index
t	Nearest-neighbor hopping amplitudes
u	Bloch states
c^\dagger, c	Fermionic creation, annihilation operators
f^\dagger, f	Flat-band projected fermionic creation, annihilation operators
Band Topology and Geometry	
Q	Quantum geometric tensor (QGT)
g	Quantum (Fubini-Study) metric
Ω	Berry curvature
\mathcal{A}	Berry connection
\mathcal{C}	Chern number

1 Electrons in a Lattice

Solids are described by lattices. The lattice sites correspond to atoms. At sufficiently low temperatures, materials assume this phase of matter to reduce entropy. Lattices assume far few symmetries than the vacuum. All continuous symmetries are lost (e.g. translation, rotation), but some discrete symmetries (e.g. reflection, discrete translation) may remain. These symmetries uniquely characterize the lattice. The lattice provides us information about the band-structure, or energy levels, of the solid, and its conductive features.

1.1 Lattices

The classification of lattices below does not use quantum mechanics. A d -dimensional **Bravais lattice** is the structure formed by a set of vectors [14]

$$\mathbf{R} = \sum_{i=1}^d n_i \mathbf{a}_i. \quad (1)$$

where $n_i \in \mathbb{Z}$, and \mathbf{a}_i are linearly independent vectors called the **primitive lattice vectors**. These vectors need not be orthogonal.¹ The choice of such vectors is not unique just as the choice of a basis for a vector space is not unique. Standard examples of Bravais lattices include the triangular and rectangular lattices.² However, not all crystals fall into this definition. Instead of referring to the locations of atoms, the Bravais lattice may instead refer to some periodic structure with additional degrees of freedom at each site. These degrees of freedom may define the locations of atoms, as is the case for the honeycomb lattice which describes graphene.

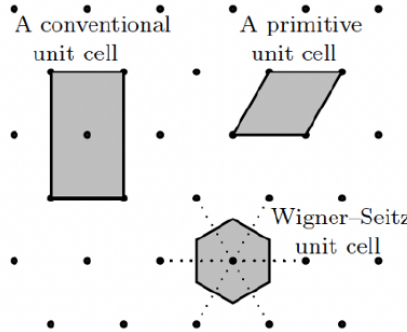


Figure 1: Generic unit cell, primitive unit cell and Wigner-Seitz unit cell of a triangular lattice [14].

The lattice is a periodic structure, and therefore has some discrete translational symmetry. We can therefore focus on a small region of the lattice which can tile the plane. The ability to tile the plane is crucial since it implies that our region captures all of the essential characteristics of the lattice, and we are free to ignore the rest of the lattice. Such a region that can tile the plane is called a unit cell. The unit cell is not unique, and there is the notion of a **primitive unit cell** with smallest area, which is also not unique. There is also the notion of the Wigner-Seitz unit cell, which is constructed by taking the intersection of the area enclosed by the perpendicular bisectors from one lattice sites to its nearest neighbors (see Figure 1).

¹In the case of orthogonal primitive lattice vectors, the lattice forms a hyper-cube.

²There are only five distinct types of Bravais lattices in two dimensions: oblique, square, triangular, primitive rectangular, and centered rectangular [14].

The lattice L is periodic, and so we can utilize standard techniques from Fourier analysis on scalar functions $F : L \rightarrow \mathbb{C}$ that shares the periodicity of the lattice, $F(\mathbf{x} + \mathbf{a}_j) = F(\mathbf{x})$ for any primitive vector \mathbf{a}_j . From physical grounds, we expect the momentum to be quantized, and the particular values it takes to be related to the type of lattice. Consider the Fourier transform

$$\tilde{F}(\mathbf{k}) = \int d^2\mathbf{x} \cdot e^{i\mathbf{k}\cdot\mathbf{x}} \cdot F(\mathbf{x}), \quad (2)$$

and analyze for which momentum \mathbf{k} this function is non-zero. Naturally, for $\tilde{F}(\mathbf{k})$ to be non-zero, we expect that the integrand must be invariant under the discrete translation, $\mathbf{x} \mapsto \mathbf{x} + \mathbf{a}_j$, which requires that $e^{i\mathbf{k}\cdot\mathbf{a}_j} = 1$. This restriction then implies the form of the so-called reciprocal lattice vectors [14],

$$\mathbf{k} = \sum_{i=1}^d n_i \cdot \mathbf{b}_i \quad (3)$$

where $n_i \in \mathbb{Z}$, and \mathbf{b}_i are the so-called primitive reciprocal lattice vectors, defined by $\mathbf{a}_i \cdot \mathbf{b}_j = 2\pi\delta_{ij}$. The reciprocal lattice vectors form a new lattice structure in momentum space called the reciprocal lattice. The primitive reciprocal lattice vectors are simply the primitive vectors of the reciprocal lattice, and we define the so-called **Brillouin zone (BZ)** to be its Wigner-Seitz unit cell. The BZ will be of primary focus, and Bloch's theorem will place a constraint on its topology [14, 7].

1.2 Bloch's theorem

For the remainder of the paper, we focus on two dimensions, $d = 2$. We follow the derivation in [14].

Suppose we have a lattice with lengths N_j along (normalized) primitive lattice vectors \mathbf{a}_j . The total number of unit cells is then simply $N = N_1 N_2$. We are interested in the properties of bulk electrons, and thus we impose periodic boundary conditions. The lattice is composed of atoms, which induce a periodic, ionic potential, $U(\mathbf{x})$. The Hamiltonian describing an electron in this lattice is then

$$H(\mathbf{r}) = \frac{\mathbf{p}^2}{2m} + U(\mathbf{r}). \quad (4)$$

We wish to understand the eigenstates of H , and we do so by utilizing its discrete translational symmetries. Discrete translation operators $T_j \equiv e^{-\mathbf{a}_j \cdot \nabla}$ commute with the Hamiltonian, and with each other, and therefore, we may construct a basis of functions that are simultaneously eigenstates of H and $T_{\mathbf{a}_j}$. In other words, the eigenstates of the Hamiltonian are eigenstates of the translation operators. We let $f(\mathbf{r})$ be an element of such a basis

$$T_{\mathbf{a}_j} f(\mathbf{r}) = \lambda_j f(\mathbf{r}), \quad H(\mathbf{r}) f(\mathbf{r}) = E f(\mathbf{r}) \quad (5)$$

where $\lambda_j^{N_j} = 1$ by noting that the periodic boundary condition imposed on the lattice requires that $T_{\mathbf{a}_j}^{N_j} = \mathbf{1}$. Therefore, λ_j must be a root of unity $\lambda_j = e^{2\pi i n_j / N_j}$, $n_j \in \{0, 1, \dots, N_j - 1\}$. We define the quasi-momentum $\mathbf{k} = \sum_{j=1}^2 n_j \mathbf{b}_j / N_j$ where \mathbf{b}_j are the primitive reciprocal vectors satisfying $\mathbf{a}_i \cdot \mathbf{b}_j = 2\pi\delta_{ij}$ and may then write $\lambda_j = e^{i\mathbf{k}\cdot\mathbf{a}_j}$, and note that λ_j are invariant under $\mathbf{k} \rightarrow \mathbf{k} + \mathbf{b}_j$. Therefore, equivalence in momentum space is equality modulo a reciprocal lattice vector and all unique momenta lie in the BZ, a discrete set of size N . This equivalence also places boundary conditions on the BZ which makes its topology that of the torus T^2 .

Returning to our problem, we can label the eigenstates of the translation operator by \mathbf{k} and label that of the Hamiltonian by a band index n . In a lattice, the energy levels are discrete and referred to as bands, similar to those of a harmonic oscillator potential, except that they are generally momentum-dependent. We have the simultaneous eigenstates

$$T_{\mathbf{a}_j} f_{n,\mathbf{k}}(\mathbf{r}) = e^{i\mathbf{k}\cdot\mathbf{a}_j} f_{n,\mathbf{k}}(\mathbf{r}), \quad H(\mathbf{r}) f_{n,\mathbf{k}}(\mathbf{r}) = E_{n,\mathbf{k}} f_{n,\mathbf{k}}(\mathbf{r}). \quad (6)$$

The former condition restricts the form of the eigenstates,

$$f_{n,\mathbf{k}}(\mathbf{r}) = \frac{1}{\sqrt{N}} e^{i\mathbf{k}\cdot\mathbf{r}} u_{n,\mathbf{k}}(\mathbf{r}), \quad u_{n,\mathbf{k}}(\mathbf{r} + \mathbf{a}_j) = u_{n,\mathbf{k}}(\mathbf{r}), \quad \int_{\Omega} d^2\mathbf{r} \cdot |u_{n,\mathbf{k}}(\mathbf{r})|^2 = 1 \quad (7)$$

where $u_{n,\mathbf{k}}(\mathbf{r})$ is called the **Bloch state** and Ω denotes the primitive unit cell. We see that the form of $f_{n,\mathbf{k}}(\mathbf{r})$ is that of a plane-wave modulated by a function periodic in the unit cell.

1.3 Topological argument for studying two dimensions

To motivate the importance of two-dimensional ($d = 2$) systems, we consider a simple argument that reveals the hidden structure of this dimension compared to $d = 1, 3$. We consider a gapped (bulk-insulating) Hamiltonian $H(\mathbf{k}) = \text{diag } \varepsilon_i(\mathbf{k})$, written in its eigenbasis. This matrix can be adiabatically transformed with unitary matrix $U(\mathbf{k})$, $\tilde{H} \equiv U^\dagger(\mathbf{k}) H(\mathbf{k}) U(\mathbf{k})$ so that the valence bands are mapped to -1 , and the conduction bands are mapped to $+1$, while maintaining the gap, and therefore the topology. With this change of basis, the Hamiltonian is transformed to $\tilde{H} = \mathbf{1}_{m \times m} \oplus (-\mathbf{1}_{(n-m) \times (n-m)})$, which is momentum-independent. Importantly, the definition of the unitary transformation $U(\mathbf{k})$ is ambiguous since we have the gauge transformation, $U(\mathbf{k}) \mapsto U(\mathbf{k}) \cdot U_{m \times m}(\mathbf{k}) \oplus U_{(n-m) \times (n-m)}(\mathbf{k})$ for any pair of unitary matrices $U_{m \times m}(\mathbf{k})$ and $U_{(n-m) \times (n-m)}(\mathbf{k})$ since the Hamiltonian is left invariant $\tilde{H} \mapsto \tilde{H}$. Therefore, the unitary matrix $U(\mathbf{k})$ is more precisely an element of the quotient group, $M \equiv U(n)/(U(m) \times U(n-m))$ where $U(n)$ is the unitary group of $n \times n$ matrices. As we are interested in the topological nature of the Hamiltonian, it is natural to consider the topology of the gauge transformations since they reveal a degree of freedom in the original problem. The appropriate object to consider is the d^{th} homotopy group

$$\pi_d(M) = \begin{cases} 0 & d = 1, 3 \\ \mathbb{Z} & d = 2 \end{cases} \quad (8)$$

which reveals non-trivial topology ($\pi_2(M) = \mathbb{Z}$) only for $d = 2$, considering $d \leq 3$. The topological invariants corresponding to \mathbb{Z} are precisely Chern numbers, $C \in \mathbb{Z}$, and therefore the only topological states that can exist in $d = 2$ (and therefore $d \leq 3$), are the quantum Hall states. With additional symmetry considerations, such as particle-hole (PH) symmetry or time-reversal symmetry, the space of gauge transformations M shrinks from further quotienting, and the homotopy groups may become more non-trivial. In the case of both aforementioned symmetries, we are left with a topological index of \mathbb{Z}_2 .

1.4 Tight-binding model

Now that we understand the importance of two dimensions, we introduce the necessary formalism and assumptions to study two-dimensional lattice models. The result of Bloch's theorem is rather intuitive. Translational symmetry implies the conservation of momentum, and therefore we can index the eigenstates with the momentum quantum number. Momentum and position are

Fourier-complements, and therefore the Bloch states have indefinite position since they have definite momentum. This manifests through the plane-wave factor attached to the real-space representation of the Bloch state. However, when one typically thinks of atomic orbitals, it is natural to envision them as localized near atoms. These localized orbitals are represented by so-called **Wannier orbitals**, $W_{n,\mathbf{R}}(\mathbf{r})$ centered at position \mathbf{R} within energy band n . These localized orbitals can be obtained as a Fourier transform of Bloch states and are orthogonal in both indices, as expected for localization. Note that simply taking a (discrete) Fourier transform of definite-momentum Bloch states does not guarantee localized orbitals. The condition of orthogonality can simply be satisfied by delocalized states that are sufficiently oscillatory. For our purposes, we justifiably assume that the lattice models we consider have localized orbitals.

With this notation of localized orbitals, we consider the most-simple non-interacting, single-particle model that reveals immense information about electron dynamics, the so-called **tight-binding model**. As the name suggests, the assumption is that we are able to construct tightly-bound, localized orbitals. Once this assumption is made, we model the kinetic energy of the electron as hopping between sites in real-space. With the language of second-quantization, (a fermion) hopping from site i to j is represented by the fermionic operator $c_i^\dagger c_j$. This representation is very intuitive since c_j annihilates a fermion at site i and c_i^\dagger creates a fermions at site j , and therefore the combined affect is an electron hopping from site i to j . If the system is time-reversal invariant, then the electron's affinity to hop from site i to j should be equal to the reverse process, hopping from site j to i , and consequently we must also include the reverse-term $c_j^\dagger c_i = (c_i^\dagger c_j)^\dagger$. With these simple building blocks, we are ready to write the Hamiltonian [7, 14]

$$H = \frac{1}{2} \sum_{i,j} (c_i^\dagger c_j + h.c.) \quad (9)$$

where $h.c.$ does Hermitian-conjugate of the first term in the summand, and the factor of $1/2$ is to account for double-counting. Note that we have not even specified a lattice yet. This model is generic to all lattice systems, although it may not accurately model the system due to the presence of interactions. Since electrons are presumably unlikely to hop across the entire lattice, a more realistic Hamiltonian would be to only consider nearest-neighbor hoppings, denoted $\langle i, j \rangle$. The procedure to solve for the energy bands (also called band-structure) and all quantities of importance is to apply the relevant unitary transformation to diagonalize the Hamiltonian. In the case of momentum-conservation, the natural unitary transformation is the Fourier transform.

As mentioned above, for a periodic structure, we have translation symmetry and therefore conservation of momentum. Similar to a particle-in-a-box, the momentum is quantized. However, unlike that scenario, there is a natural highest-momentum given by the inverse of the lattice spacing, $k = 2\pi(N - 1)/(a_0 N)$ where a_0 is the lattice spacing, and N is the length. In general, the momenta can assume values $k_n = 2\pi n/(a_0 N)$ for $n \in \{0, 1, \dots, N - 1\}$. This result can be trivially generalized to higher dimensions, where the momentum in each direction is quantized accordingly.

To demonstrate this procedure, we compute the band-structure of a one-dimensional lattice with lattice spacing a_0 , and nearest-nearest neighbor hopping amplitude $-t$ with $t > 0$. The resulting Hamiltonian can be written as [14]

$$H = -t \sum_{j=1}^{N-1} (c_j^\dagger c_{j+1} + h.c.) \quad (10)$$

where we impose periodic boundary conditions (PBC) by requiring that site N is equivalent to site 1, forming a circular chain of N lattice sites. We then Fourier expand each fermion operator using the expansion, $c_j^\dagger = \frac{1}{\sqrt{N}} \sum_k e^{-i(ja_0) \cdot k} c_k^\dagger$, obtaining [14]

$$\begin{aligned} H &= -\frac{t}{N} \sum_{j=1}^{N-1} \sum_{k,k'} (e^{-i(ja_0) \cdot k + i((j+1)a_0) \cdot k'} c_k^\dagger c_{k'}' + h.c.) \\ &= -t \sum_k (e^{ia_0 k} c_k^\dagger c_k + h.c.) \\ &= -2t \sum_k \cos(ka_0) c_k^\dagger c_k \end{aligned} \tag{11}$$

and therefore the band-structure (eigenvalues) can simply be read off since the Hamiltonian is diagonal,³, $\varepsilon(k) = -2t \cos(ka_0)$. In the second line, we used the identity $\sum_{\mathbf{R}} e^{i\mathbf{R} \cdot \mathbf{k}} = N \cdot \delta_{\mathbf{k}}$.

In the interacting case, the procedure to diagonalize the Hamiltonian also requires transforming each of the real-space fermion operators into momentum space. However, interacting-Hamiltonians, such as a two-body interaction, does not have a nice analytic form and typically requires numerical diagonalization.

The number of bands we obtain is equal to the number of non-translational degrees of freedom the model contains. The square lattice we considered earlier is the most simple two-dimensional lattice, and does not have any additional degrees of freedom, and so the result we obtained from applying the tight-binding model was only one band, $\varepsilon(\mathbf{k})$. On the other hand, graphene is a honeycomb lattice which is composed of a single triangular Bravais lattice, but with the addition of a sublattice index. A triangular lattice can map the centers \mathbf{R} of the unit cells (honeycombs), and for each unit cell, the lattice sites are located at positions $\mathbf{R} + \mathbf{r}_\alpha$ where $\alpha = A, B$ denotes the sublattice index. The Hamiltonian becomes a 2×2 matrix in the sublattice index, and solving the tight-binding model results in two bands, the **valence band** (lower) and the **conduction band** (higher). If the bands do not intersect anywhere in the BZ, and the Fermi level is located in the gap, the model is said to be gapped. As the name suggests, electrons in the valence band are localized to the atom's valence (outermost) orbitals, and therefore do not contribute to transport. Any fully-filled band is a valence band since unoccupied states are required to achieve transport [7].⁴ At charge neutrality (undoped), transport can be achieved by exciting an electron from the valence band to the conduction band by providing it with the necessary energy to excite over the band gap.

2 Integer Quantum Hall Effect

We shift gears to another realm of condensed matter physics, one without a single mention of lattices, but still residing on a two-dimensional solid plane. Of course, lattices are still present since all solids have a lattice structure, but the lattice becomes irrelevant to the physics in the appropriate regime, and can be ignored entirely. However, in an absolute sense, the lattice exists and even breaks certain symmetries. Consider for example that a lattice has far fewer symmetries than free space. The symmetries of a lattice are discrete, a subset of the continuous symmetries

³Since we do not have any scattering terms ($c_k^\dagger c_{k'}$ for $k \neq k'$) the Hamiltonian simply decomposes into Bloch diagonal form, $H = \bigoplus_k H_k$ where $H_k = -2t \cos(ka_0)$ is a 1×1 matrix (scalar).

⁴The choice of calling a certain band a valence band presumes that it is (approximately) completely filled and cannot host transport.

of real space (e.g. rotation, translation). Therefore, after we start neglecting the lattice, note that from a fundamental point of view, we do not have any continuous symmetry that an otherwise free space might contain.

We provide an overview to the **integer quantum Hall effect (IQHE)**, a phase of matter that is not described by the order parameter in the Landau theory of phase transitions. It is in this way that the IQHE marks the first revolutionary step away from Landau's theory, which was commonly believed to be able to classify all phases of matter. To recall, the order parameter is a continuous function which shares the same symmetries as the model. It is used to track a key property of a model and behaves non-trivially near a phase transition due to spontaneous symmetry breaking. In the Ising model for instance, below the critical temperature, the system spontaneously breaks \mathbb{Z}_2 symmetry and the magnitude of the magnetization (order parameter) becomes non-zero. The IQHE is an example of a phase in which topological order is responsible for its robustness (in zero temperature), instead of a continuous parameter. To understand the fundamental difference between topological order and the Landau theory, consider an ordinary sphere S^2 , and recall the Gauss-Bonnet theorem which relates the Gaussian curvature K of the manifold ($M = S^2$) to its Euler characteristic $\chi(M) \in \mathbb{Z}$, a topological quantity [3],

$$\chi(M) = \frac{1}{2\pi} \int_M d^2k \cdot K \quad (12)$$

where the above equation holds for any smooth two-manifold M with no boundary, $\partial M = 0$.⁵ The Gaussian curvature is a smooth function, and is intrinsically tied to the geometry of the manifold, but no matter how the curvature is smoothly deformed, the Euler characteristic will remain unchanged. Topological order is an immensely strong constraint.

2.1 Classical Hall effect

We describe the conductivity and resistivity as rank-2 tensors which obey Ohm's law⁶ $j_\mu = \sigma_{\mu\nu} E_\nu$, $E_\mu = \rho_{\mu\nu} j_\nu$, $\sigma_{\mu\nu} = (\rho^{-1})_{\mu\nu}$. Consider static electric and magnetic fields $\mathbf{E} = E\hat{\mathbf{x}}$, $\mathbf{B} = B\hat{\mathbf{z}}$ acting on a planar surface ($\hat{x}\hat{y}$ plane). In the absence of an electron field, we expect cyclotron motion due to the magnetic field. However, note that in the steady state ($\mathbf{F} = 0$), the Lorentz force law implies that there is also the contribution from $\mathbf{E} \times \mathbf{B}$ drift, which results in a current perpendicular to both applied fields [7]. Due to the presence of this quantity we obtain the Hall conductivity $\sigma_{xy} = n_e q/B$ and vanishing longitudinal conductivity (cyclotron motion does not contribute to conductivity since it is localized). This effect is known as the classical Hall effect, and is not terribly interesting. When you first read about this effect for the first time, it may surprise you that applying an electric field produces a current in a perpendicular direction, but once you understand the role of the magnetic field, all becomes quaint. One crucial point to notice is that the Hall conductivity σ_{xy} is a continuous parameter, and is not quantized in any way. This will change when we compute the Hall conductivity in the quantum mechanical regime.

2.2 Landau Levels

A brief overview of electromagnetism in quantum mechanics will be provided along with Landau levels and the corresponding electron wave functions, and quantized Hall resistivity. We also explain

⁵This equation will pop up a few more times as an analogy to make topological quantities more familiar to the reader.

⁶Note that this is a slight generalization to the introductory treatment of these quantities as scalars, but this treatment is justified naturally.

the role of disorder in the size of the plateaus. Throughout this section, we do not consider Coulomb interactions between the electrons. This inter-electron interaction will become crucial to the discussion of the fractional quantum Hall effect in the next section. We follow the derivations in [7].

Consider a particle of charge q and mass m in an applied electromagnetic field with vector potential \mathbf{A} and scalar potential ϕ . The electromagnetic field couples to the particle through the minimal coupling

$$H = \frac{1}{2m}(\mathbf{p} - q\mathbf{A})^2 + q\phi \quad (13)$$

where $\mathbf{p} = -i\hbar\nabla$ is the momentum operator and satisfies the commutation relation $[x_\mu, p_\nu] = i\hbar\delta_{\mu\nu}$. The same Hamiltonian describes classical electromagnetism, except that the momentum and electromagnetic potentials are functions instead of operators. We naturally require that observables are left unchanged under any gauge transformation $\mathbf{A} \mapsto \mathbf{A} + \nabla\Lambda$, $\phi \mapsto \phi - \partial_t\Lambda$ which constrains the Hamiltonian and wave function to transform as $\psi \mapsto U\psi$, $H \mapsto UHU^\dagger$ where $U = \exp(iq\Lambda/\hbar)$ is a unitary operator.

We now return to the planar electron in a perpendicular magnetic field $\mathbf{B} = B\hat{\mathbf{z}}$. For the moment, we do not consider any electric field. The (quantum) Hamiltonian can be written

$$H = \frac{1}{2m}(\mathbf{p} - q\mathbf{A})^2, \quad (14)$$

and we solve for the velocity using the Heisenberg equation of motion $\mathbf{v} \equiv \dot{\mathbf{r}} = \frac{i}{\hbar}[H, \mathbf{r}] = \frac{1}{m}(\mathbf{p} - q\mathbf{A}) \equiv \mathbf{\Pi}$ where we defined the kinetic momentum $\mathbf{\Pi} \equiv m\mathbf{v} = \mathbf{p} - q\mathbf{A}$ to be the velocity above scaled by the electron mass. Note that $\mathbf{\Pi}$ is not the momentum of the electron. It includes both the electron's momentum as well as momentum in the electromagnetic field, the combination of which is conserved, $\dot{\mathbf{\Pi}} = 0$, and not either contribution individually. The kinetic momentum obeys the commutation relations $[\Pi_x, \Pi_y] = i\hbar eB = -i\hbar^2/l_B^2$ where we introduce the magnetic length $l_B = \sqrt{\hbar/eB}$.

For typical laboratory magnetic fields (e.g. $B = 6\text{T}$), the magnetic length is approximately 10nm. While it might seem small, it is significantly larger than the typical lattice spacing (e.g. graphene lattice spacing is a few angstrom (10^{-10} m)). It turns out that the magnetic length is the characteristic length scale of the wave function, and therefore, the wave function is nearly 10^2 times as wide as the typical lattice spacing. It is for this reason that we can effectively ignore the lattice and treat the plane with the same symmetries as free space.

Although it may seem that we are more or less following the same derivation as the classical case, there is one crucial aspect of electromagnetism in quantum mechanics that has no classical analogue. Consider a confined tube of magnetic flux flowing along the \hat{z} axis. According to the Lorentz force law, we would expect that outside the tube, a charged particle would not experience any electromagnetic force, and that would be correct. Although the magnetic field is confined to the tube, the vector potential is non-zero. This little note should not matter since the vector potential is solely used to organize the magnetic and scalar potential into a single quantity, and at the end of the day, the Lorentz force law dictates the dynamics of charged particles. In quantum mechanics, the story is drastically different. The charged particle is directly affected by the tube even when it is outside the tube due to the non-triviality of the vector potential. This phenomenon is known as the Aharonov-Bohm effect and will be an important aspect when we consider interactions in the next section on the fractional quantum Hall effect. Fundamentally, it arises because the vector

potential is elevated to an operator in quantum mechanics, and causes non-triviality of translation operators. The details are not important for our discussion.

So far, we have not accomplished much, the Hamiltonian can be written as $H = \boldsymbol{\Pi}^2/2m$ which looks like the free-particle Hamiltonian, $H = \mathbf{p}^2/2m$. However, if we look a little closer, we will notice that while the momentum operators commute, $[p_i, p_j]$, the kinetic momentum operators do not commute, $[\Pi_x, \Pi_y] \propto 1$. Therefore, the Hamiltonian is algebraically equivalent to that of a harmonic oscillator (where $[a, a^\dagger] \propto 1$). This motivates us to solve the problem in terms of ladder operators just as the harmonic oscillator is solved. We introduce the ladder operators (unitary transformation)

$$a = \frac{l}{\sqrt{2}\hbar}(\Pi_x + i\Pi_y), \quad a^\dagger = \frac{l}{\sqrt{2}\hbar}(\Pi_x - i\Pi_y) \quad (15)$$

which satisfy $[a, a^\dagger] = 1$. Using these cleverly-defined operators, we can rewrite the Hamiltonian as a harmonic oscillator and obtain its energy levels

$$H = \hbar\omega_c \left(a^\dagger a + \frac{1}{2} \right), \quad \varepsilon_n = \hbar\omega_c \left(n + \frac{1}{2} \right) \quad (16)$$

where $n \in \mathbb{Z}_{\geq 0}$. The energy levels are commonly referred to as Landau levels. Since the term $a^\dagger a$ effectively counts the number of terms ($a^\dagger a |n\rangle = n|n\rangle$), the eigenstates can be written as $|n\rangle \equiv 1/\sqrt{n!}(a^\dagger)^n |0\rangle$. It is remarkable that the Landau levels have such simple form and are even independent of the particle's momentum.

All of the above calculations did not rely on a choice of gauge. To be able to write down eigenstates, we now consider the symmetric gauge $\mathbf{A} = \mathbf{B} \times \hat{\mathbf{r}}/2 = -By/2\hat{x} + Bx/2\hat{y}$ for the rest of the calculations, taking advantage of the rotational symmetry of the model. Given this gauge, we can expand the (gauge-invariant) position operator

$$\hat{\mathbf{r}} = \mathbf{R} + l_B^2 \hat{\mathbf{z}} \times \boldsymbol{\Pi} \quad (17)$$

where the first term, \mathbf{R} is the so-called **guiding-center** and the second term is the Landau orbit. The guiding-centers commute with the kinetic momenta $[R_i, \pi_j] = 0$. Consequently, the kinetic momenta and guiding-centers can be measured simultaneously. The guiding-centers physically correspond to the centers of the quantum-mechanical analogue of cyclotron orbits. Since its components do not commute, $[R_x, R_y] = -il_B^2$, there is some ambiguity in where exactly the center is located. Intuitively, due to translational invariance of the model ($[\mathbf{R}, H] = 0$), the energy is independent of the guiding-center, leading to a massive degeneracy in each Landau level. This degeneracy can be easily quantified. Due to the non-commutative geometry, the smallest discernible unit area corresponds to a disk of size $2\pi l_B^2$. Therefore, we can partition the area of the sample A into a grid of unit-areas to obtain a degeneracy of approximately $A/(2\pi l_B^2)$ (or the degeneracy per unit area is $(2\pi l_B^2)^{-1}$). As the magnetic length (the only characteristic length scale of the problem) decreases (increasing magnetic field), the degeneracy increases. Although the behavior is subtle, it implies that the electrons, assumed to be point-like particles in quantum mechanics, now take up space so that the entire sample can be saturated with electrons.

Since we are taking advantage of the symmetric gauge, we can more easily define quantities which rely on rotational symmetry such as angular momentum, which can be expressed as

$$L_z \equiv -i\hbar\partial_\phi = -\frac{\hbar^2}{2l_B^2}\mathbf{R}^2 + \frac{l_B^2}{2\hbar}\boldsymbol{\Pi}^2, \quad (18)$$

an intriguing quantity. Strangely, the angular momentum is dependent on the guiding-center, with arbitrary choice of origin. Due to rotational symmetry ($[L_z, H] = 0$), each Landau level is degenerate with respect to angular momentum. Since the angular momentum is deeply tied with the guiding-centers, and the guiding-centers obey harmonic oscillator commutation relations, we can define the so-called angular momentum raising and lowering operators

$$b = \frac{1}{\sqrt{2l}}(X - iY), \quad b^\dagger = \frac{1}{\sqrt{2l}}(X + iY) \quad (19)$$

which satisfy the commutation relations $[b, b^\dagger] = 1$, $[a, b] = [a^\dagger, b^\dagger] = 0$. We can also rewrite the angular momentum operator as $L_z = \hbar(a^\dagger a - b^\dagger b)$, which exactly mimics the expression for angular momentum above, with the guiding-center and kinetic momenta replaced by the a and b raising/lowering operators respectively. Since we are working in the symmetric gauge, and the system is rotationally invariant, it is expected that angular momentum is a good quantum number, and so we can use it to label the eigenstates. The (orthonormal) eigenstates of the Hamiltonian can be written

$$|n, m\rangle = \frac{1}{\sqrt{(nm)!}}(a^\dagger)^n(b^\dagger)^m|0\rangle \quad (20)$$

where the n index denotes the Landau level index, and the m index denotes angular momentum.

The angular momentum operator can also be written as $L_z = (\hat{\mathbf{r}} \times \hat{\mathbf{p}})_z = i\hbar(x\partial_y - y\partial_x) = \hbar(z\partial - \bar{z}\bar{\partial})$ where we opt for complex notation, $\partial = \partial_z = \partial_x + i\partial_y$. A simple computation shows that $L_z z^m \cdot e^{-\frac{1}{4}|z|^2} = \hbar m \cdot z^m e^{-\frac{1}{4}|z|^2}$, and therefore $\psi_m(z) \equiv z^m e^{-\frac{1}{4}|z|^2}$ is an eigenstate of L_z with eigenvalue $\hbar m$. It turns out that this state is also in the **lowest Landau level (LLL)**.

Now that we understand the energy levels of the Hamiltonian and the origin of their degeneracies, we solve for the eigenstate wave functions. We express the ladder operators in real space [5]

$$a = -\frac{i}{\sqrt{2}}(z + \bar{\partial}), \quad b = \frac{1}{\sqrt{2}}(\bar{z} + \partial) \quad (21)$$

where we have defined the complex variable $z = x - iy$ and its conjugate $\bar{z} = x + iy$. We can solve for the wave function in the LLL with zero angular momentum ($n = m = 0$) by solving the differential equation $a|0, 0\rangle = b|0, 0\rangle = 0$. We obtain the $|0, 0\rangle$ wave function [7, 5]

$$\psi_{00}(z) \equiv \langle z|0, 0\rangle = \frac{1}{\sqrt{2\pi l}}e^{-|z|^2/4} \quad (22)$$

and can obtain higher level wave functions by applying the raising operators a^\dagger, b^\dagger . The LLL wave function with angular momentum m can be expressed as [7, 5]

$$\psi_{0m}(z) = \frac{1}{\sqrt{2\pi 2^m m! l}} z^m e^{-|z|^2/4} \quad (23)$$

which corresponds to an electron (approximately) localized on an annular region of minimum radius $r_m = \sqrt{2ml}$, maximum radius r_{m+1} , and area $A = \pi(r_{m+1}^2 - r_m^2) = 2\pi l^2$. Note that the area occupied by each electron in the LLL is constant, irrespective of angular momentum. This is the same result we derived from the non-trivial commutation relation of the guiding-centers. This area occupied by single electrons holds for higher Landau levels as well. Note that the magnetic flux that penetrates the area occupied by a single electron is a constant $BA = B \cdot 2\pi l^2 = h/e = \Phi_0$ called the flux quantum. In other words, there is precisely one electron state per flux quantum per

Landau level [7, 5]. Increasing the magnetic field increases the number of electron states by raising maximum angular momentum. Thus there are $N_\Phi = \Phi/\Phi_0$ angular momentum states in the LLL where $\Phi = BA$ is the total flux penetrating the sample. Although we derived this result in the symmetric gauge with a disk geometry, we can obtain the same result in the Landau gauge⁷ with a rectangular geometry.

The wave function will be of central importance when we discuss the FQH effect. Note that since the Schrodinger equation is linear, we can take linear combinations of the LLL states ψ_{0m} to generate new eigenstates. Since ψ_{0m} contains the factor z^m , the wave function $\psi(\mathbf{r}) = f(z) \cdot e^{-|z|^2/4}$ is also an eigenstate of the LLL where $f(z)$ is holomorphic (complex-differentiable). For higher Landau levels, the prefactor to the Gaussian becomes partly anti-holomorphic (proportional to \bar{z}), and becomes difficult to deal with. The holomorphic degree of freedom of the LLL will be used to construct FQH states down the road.

2.3 Hall conductance (naive calculation)

So far, we have computed the eigenvalues and eigenstates of the Hamiltonian, $H = \mathbf{\Pi}^2/2m$, and now we wish to study the effects of introducing an in-plane electric field, $\mathbf{E} = E\hat{x}$. With the introduction of this field, we have broken rotational symmetry and therefore we can no longer take advantage of the symmetric gauge⁸. We instead use the Landau gauge $\mathbf{A} = Bx\hat{y}$, and obtain the Hamiltonian [7]

$$H = \frac{1}{2m}(p_x^2 + (p_y - qBx)^2) + qEx. \quad (24)$$

It is simple to see that $[H, p_y] = 0$ and so we have the eigenstate ansatz, $\varphi(\mathbf{r}) = e^{ik_y y}\psi(x)$, from which we obtain the expanded Hamiltonian $H = p_x^2 + (\hbar k_y - qBx)^2 + qEx$. Applying this Hamiltonian to an eigenstate $\psi(x)$ with energy ε , after some simplification (completing the square), we obtain

$$\left(\frac{1}{2m}p_x^2 + \frac{1}{2}m\omega_c^2(x - X)^2 \right) \psi(x) = \left(\varepsilon_x - qEX - \frac{1}{2}m(E/B)^2 \right) \psi(x). \quad (25)$$

where $X = k_y l_B^2 + \frac{qE}{m\omega_c^2}$, and ω_c is the cyclotron frequency. The left-hand-side is the Hamiltonian of a harmonic oscillator centered at position X , and the right-hand-side is a constant, a shift in the energy. The energy levels can then be easily solved [7]

$$\varepsilon_{n,X} = \hbar\omega_c \left(n + \frac{1}{2} \right) + qEX + \frac{1}{2}mE/B \quad (26)$$

where the first term is the harmonic oscillator energy, the second term is the scalar potential, and the last term is due to the $\mathbf{E} \times \mathbf{B}$ drift. A naive computation of the expectation values of the current operators shows that $\langle \psi | j_x | \psi \rangle = 0$, $\langle \psi | j_y | \psi \rangle = E/B$ from which we obtain $\sigma_{xy} = n_e q/B$ and $\sigma_{xx} = 0$.⁹ So far, all of our results have been a repeat of the classical treatment. The Hall conductivity is not yet quantized. We have to consider the theory a little more carefully to derive the quantization.

⁷The Landau could also have been used to solve this problem, resulting in wave functions which are translationally invariant in one direction, but the physics is the same.

⁸Of course, we could still use the symmetric gauge if we wanted, but angular momentum is no conserved and therefore cannot index the eigenstates, and so its not a gauge that accurately captures the model.

⁹We used that $j_y = n_e q/B$.

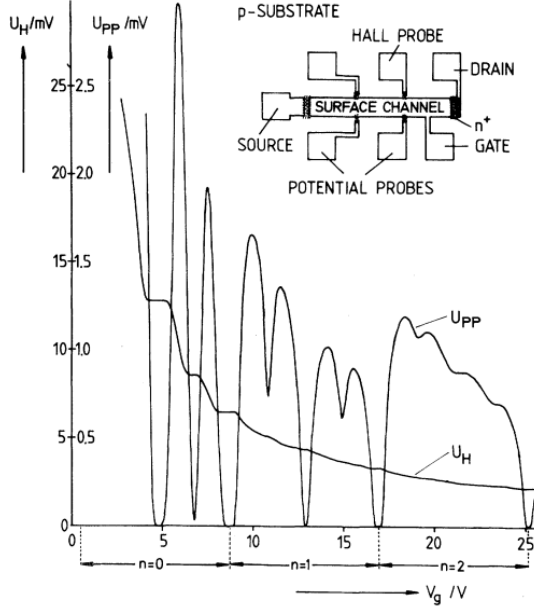


Figure 2: Hall and longitudinal conductivity as a function of gate voltage (filling factor). The magnetic field is held constant at 18T, and the temperature is 1.5K, as measured by von Klitzing [11].

2.4 Band geometry

We now develop the theory of band topology and geometry to better understand the global and local properties of bands. Quantum mechanics is built on Euclidean space. The wave functions $\psi(\mathbf{x}, t)$ take as variable the position $\mathbf{x} \in \mathbb{R}^3$ and time. There is no mention of a non-trivial metric or topology. However, with the introduction of a Hamiltonian, we obtain a band-structure, or more generally an eigenspace (manifold) which may have non-trivial geometry and topology. It turns out that both Landau levels and some lattice models (without magnetic field) possess remarkable geometric and topological properties which we will now develop the formalism to explore.

We consider a parameter-dependent non-degenerate Hamiltonian $H(\lambda_\mu)$ and consider a state $|\psi(\lambda_\mu)\rangle$ in the Hilbert space. In the case we are interested, this parameter is simply the momentum, which we take as a good quantum number due to translational invariance.¹⁰ We are in search of a metric on the Hilbert space that will allow us to define a notion of distance, capturing both differences in phase and magnitude. The wave function can be expanded about the parameter λ_μ to second-order in the displacement $d\lambda_\mu$ [4]

$$|\psi(\lambda_\mu + d\lambda_\mu)\rangle = |\psi(\lambda_\mu)\rangle + d\lambda^\mu \cdot |\partial_\mu \psi\rangle + \frac{1}{2} d\lambda^\mu d\lambda^\nu \cdot |\partial_\mu \partial_\nu \psi\rangle + \mathcal{O}(d\lambda^3), \quad (27)$$

where we make use of tensor notation and assume Einstein summation where appropriate. Using

¹⁰For a finite lattice with periodic boundary conditions (forming a torus), we have a discrete number of distinct momenta in the BZ. As the lattice-size increases and is taken to be infinite, grid of momenta points forms a continuum in the BZ. It is in this sense that we can consider the smooth parameter λ_μ .

only the first-order expansion, we compute the infinitesimal distance between nearby states [4]

$$\begin{aligned} ds^2 &\equiv |\psi(\lambda_\mu + d\lambda_\mu) - \psi(\lambda_\mu)|^2 \\ &= |d\lambda^\mu \cdot |\partial_\mu \psi\rangle|^2 \\ &= \langle \partial_\mu \psi | \partial_\nu \psi \rangle \cdot d\lambda^\mu d\lambda^\nu \equiv (\gamma_{\mu\nu} + ip_{\mu\nu}) \cdot d\lambda^\mu d\lambda^\nu \end{aligned} \quad (28)$$

where in the last step we simply defined $\gamma_{\mu\nu}$ and $p_{\mu\nu}$ as the real and imaginary parts of $\langle \partial_\mu \psi | \partial_\nu \psi \rangle$ respectively.¹¹ Note that since $\langle \partial_\mu \psi | \partial_\nu \psi \rangle = \langle \partial_\nu \psi | \partial_\mu \psi \rangle^*$, we must have that $\gamma_{\mu\nu}$ is a symmetric tensor and $p_{\mu\nu}$ is an anti-symmetric tensor. Therefore, the distance reduces to $ds^2 = \gamma_{\mu\nu} \cdot d\lambda^\mu d\lambda^\nu$ since the anti-symmetry of $p_{\mu\nu}$ eliminates it under summation. We might be quick to then claim that $\gamma_{\mu\nu}$ is the metric we are seeking, but it is not gauge-invariant. Indeed, the gauge transformation $|\psi(\lambda_\mu)\rangle \mapsto e^{i\Lambda(\lambda_\mu)} |\psi(\lambda_\mu)\rangle$ transforms the above quantities

$$\gamma_{\mu\nu} \mapsto \gamma_{\mu\nu} - \mathcal{A}_\mu \partial_\nu \Lambda - \mathcal{A}_\nu \partial_\mu \Lambda + \partial_\mu \Lambda \partial_\nu \Lambda, \quad p_{\mu\nu} \mapsto p_{\mu\nu} \quad (29)$$

where $\mathcal{A}_\mu \equiv i \langle \psi | \partial_\mu \psi \rangle$ is the **Berry connection** and transforms as $\mathcal{A}'_\mu = \mathcal{A}_\mu + \partial_\mu \Lambda$. We will return to the Berry connection shortly and explain its physical significance after we have developed the quantum geometric tensor and Berry curvature. By noting how the Berry connection transforms under gauge transformations, we define the symmetric, gauge-invariant so-called **quantum (Fubini-Study) metric** tensor [4]

$$g_{\mu\nu} = \gamma_{\mu\nu} - \mathcal{A}_\mu \mathcal{A}_\nu. \quad (30)$$

This metric defines a notion of distance between states on the projected Hilbert space in which we compare states modulo (without) their phase, so-called quantum rays. That is, we are quantifying the distance between states purely in terms of changes in their magnitude rather than their phase. Since we are only considering magnitudes, this quantity is manifestly gauge-invariant. On the other hand, $p_{\mu\nu}$, which is already gauge-invariant, only takes into consideration the difference in phase.

To understand the significance of the quantum metric, we compute the (squared) overlap with the unperturbed state, only considering changes in magnitude,

$$\begin{aligned} |\langle \psi(\lambda) | \psi(\lambda_\mu + d\lambda_\mu) \rangle|^2 &= \left| 1 + d\lambda^\mu \cdot \langle \psi(\lambda) | \partial_\mu \psi \rangle + \frac{1}{2} d\lambda^\mu d\lambda^\nu \cdot \langle \psi(\lambda) | \partial_\mu \partial_\nu \psi \rangle \right|^2 \\ &= 1 - (\text{Re}(\langle \partial_\mu \psi | \partial_\nu \psi \rangle) + \langle \psi | \partial_\mu \psi \rangle \langle \psi | \partial_\nu \psi \rangle) \\ &= 1 - (\gamma_{\mu\nu} - \mathcal{A}_\mu \mathcal{A}_\nu) \cdot d\lambda^\mu d\lambda^\nu \\ &= 1 - g_{\mu\nu} \cdot d\lambda^\mu d\lambda^\nu, \end{aligned} \quad (31)$$

from which we obtain the overlap

$$|\langle \psi(\lambda) | \psi(\lambda_\mu + d\lambda_\mu) \rangle| = 1 - \frac{1}{2} g_{\mu\nu} \cdot d\lambda^\mu d\lambda^\nu \quad (32)$$

using $\sqrt{1-x} \approx 1-x/2$ [4]. Note that this term does not contain any terms with a single derivative, and so it is analogous to the Gaussian curvature of a manifold. To unify all of the quantities, we define the **quantum geometric tensor (QGT)**

$$Q_{\mu\nu} = \langle \partial_\mu \psi | P_\psi^\perp | \partial_\nu \psi \rangle \quad (33)$$

¹¹We often omit writing the dependence on the parameter λ_μ when it is clear from context.

where $P_\psi^\perp = 1 - |\psi\rangle\langle\psi|$ projects onto the maximal subspace not including $|\psi\rangle$. This object captures all geometric information of the normalized family of states $|\psi(\lambda)\rangle$. In particular, the previous quantities can be recovered [4]

$$g_{\mu\nu} = \text{Re}(Q_{\mu\nu}), \quad p_{\mu\nu} = \text{Im}(Q_{\mu\nu}), \quad (34)$$

where it is natural that the metric keeping track of the phase, $p_{\mu\nu}$ is the imaginary part of the QGT since phases are complex exponentials.

While the quantum metric is probably a novel quantity for many undergraduate students, the metric $p_{\mu\nu}$ is closely related to the **Berry phase**. As a brief review, the Berry phase ϕ is a time-independent phase that a particle accrues upon adiabatic transport,¹²

$$\phi = \oint_{\gamma} d\lambda^{\mu} \cdot \mathcal{A}_{\mu} \quad (35)$$

where $\mathcal{A} \equiv i\langle\psi|\partial_{\mu}\psi\rangle$ is the Berry connection we encountered earlier. The Berry phase is only gauge-invariant if we assume that γ is a closed loop. In addition, while the Berry connection is not itself gauge-invariant (and is therefore not an observable), it can be differentiated to obtain the gauge-invariant **Berry curvature** $\Omega_{\mu\nu} \equiv \partial_{\mu}\mathcal{A}_{\nu} - \partial_{\nu}\mathcal{A}_{\mu} = -2\text{Im}\langle\partial_{\mu}\psi|\partial_{\nu}\psi\rangle$. Using the Berry curvature, which is basically an application of Stokes' theorem, we can rewrite the Berry phase as $\phi = \int_{\Gamma} d\lambda^{\mu} d\lambda^{\nu} \cdot \Omega_{\mu\nu}$ where γ is the boundary of the two-dimensional submanifold Γ , $\partial\Gamma = \gamma$. Upon being adiabatically transported around path γ , the wavefunction obtain a phase $e^{i\phi}$, an observable quantity. The Berry phase, which is also known as the geometric phase, is a quantity unlike the dynamical phase $e^{ist/\hbar}$ which is time-dependent. Rather, the Berry phase is only dependent on the geometry of the energy eigenspace, and the (adiabatic) path taken in parameter-space.

Since the Berry curvature captures information about how the geometric phase evolves locally, it is natural that it is related to the metric we derived earlier. Indeed, note that

$$\Omega_{\mu\nu} = \partial_{[\mu} A_{\nu]} = i\langle\partial_{[\mu}\psi|\partial_{\nu]}\psi\rangle = i(Q_{\mu\nu} - Q_{\nu\mu}) = 2\text{Im}(Q_{\mu\nu}) = -2p_{\mu\nu} \quad (36)$$

where we used that $Q_{\nu\mu} = \gamma_{\nu\mu} + ip_{\nu\mu} = \gamma_{\mu\nu} - ip_{\mu\nu} = Q_{\mu\nu}^*$. In literature, the Berry curvature is conventionally used over the metric $p_{\mu\nu}$. In all, the QGT captures the geometry of the band, which provides us information on how the state evolves under adiabatic transport.

We take a mathematician's perspective to say that the so-called **Chern number** [7, 5, 14, 4]

$$\mathcal{C} = \frac{1}{2\pi} \int_{\text{BZ}} d^2k \cdot \Omega_{\mu\nu}(k) = -\frac{1}{\pi} \int_{\text{BZ}} d^2k \cdot \text{Im}(Q_{\mu\nu})(k). \quad (37)$$

can only take integer values, a result from differential geometry. The Chern number represents the obstruction of defining the wave function globally on the BZ as opposed to using charts. If we can define the wave function globally, then integrating the Berry curvature (which is now also defined globally using a single chart) over a closed manifold¹³ will vanish. In some respect, the higher the Chern number, the harder it is to globally define the wave function using a single chart, and the more topological the system becomes. It is not at all clear what physical significance the Chern number possesses, if any, and for now just seems to be a neat topological invariant of the energy eigenspace. We will investigate the physical significance in the next section.

¹²We assume that the eigenstate $|\psi\rangle$ is in a non-degenerate eigenspace.

¹³Recall that the BZ is topologically equivalent to the torus, a closed manifold.

Note that the expression for the Chern number as an integral of a curvature term is reminiscent of the Gauss-Bonnet theorem in differential geometry [3],

$$\chi(M) = \frac{1}{2\pi} \int_M d^2k \cdot K \quad (38)$$

where K is the Gaussian curvature (closely related to the manifold's metric), $\chi(M)$ is a topological invariant of the manifold known as the Euler characteristic, and M is a compact 2-manifold with no boundary, $\partial M = 0$. The Chern number is indeed a sort of highly non-trivial generalization of this theorem called the Chern-Gauss-Bonnet theorem, where we instead consider so-called vector bundles on a manifold instead of the manifold's intrinsic curvature.

Apart from appeal to organization, it seems artificial that we combined our two metrics, g and p , into the QGT. Mathematically, the quantum metric g is a geometric property of the tangent bundle of the eigenspace manifold, and p (or the Berry curvature) is a property of the U(1) principle fiber bundle. This mathematical jargon is not necessary to understand that they capture different geometric properties of the eigenspace manifold. However, they are linked together through the QGT. To see this, consider two conveniently-chosen states, $|\alpha_i\rangle \equiv P_\psi^\perp |\partial_i \psi\rangle$ for $i = 1, 2$. These states are closely connected to the QGT, as $\langle \alpha_i | \alpha_j \rangle = Q_{ij}$, using that the projection operator is idempotent. Using the Cauchy-Schwarz Inequality, we obtain $Q_{ii}Q_{jj} \geq Q_{ij}$, which if we assume a two-dimensional parameter space (as is the case of the two-dimensional lattice with parameter $\mathbf{k} \in \mathbb{R}^2$), is equivalent to the positive semi-definiteness of the QGT ($\det Q \geq 0$). If we substitute the geometric tensor and the Berry curvature for the QGT ($Q_{ii} = g_{ii}$, $|Q_{ij}|^2 = g_{ij}^2 + \Omega_{ij}^2/4$), we obtain $g_{ii}g_{jj} - g_{ij}^2 \geq \Omega_{ij}^2/4$. Taking $i = 1, j = 2$, we finally arrive at

$$\frac{1}{4}|\Omega_{12}|^2 \leq \det g \quad (39)$$

which places an upper bound on the Berry curvature, or a lower bound on the quantum metric due to each other. The quantum metric g describes how the eigenspace manifold curves in space, and can be used to compute the volume-form,¹⁴ $\sqrt{\det g}$, which is used as the integration-measure. We can compute the total volume of the manifold, $\text{vol}_g \equiv \int d^2\lambda \cdot \sqrt{\det g}$. Integrating both sides of the above inequality, we obtain

$$\mathcal{C} \leq \text{vol}_g/\pi, \quad (40)$$

an upper bound on the Chern number. The usefulness of the quantum metric does not peak at upper-bounding the Chern number. We will return to the quantum metric when discussing interactions in the Chern insulator.

2.5 Geometry of Landau levels

We still have not explored the physical interpretation of the Chern number, or the geometry in general. Before we do so, let us naively compute (cite) the geometric and topological quantities for Landau levels. It turns out that Landau levels have a remarkably simple geometric structure.¹⁵ For the m^{th} Landau level (MLL), the quantum metric is constant and has a diagonal form, $g_{xx} = g_{yy} = (m + 1/2)/|B|$, $g_{xy} = 0$, and the Berry curvature is also constant $\Omega_{xy} = -1/B$ where B denotes the magnitude of the magnetic field, and is negative for \mathbf{B} pointing along $-\hat{z}$, the physical

¹⁴Since we are assuming a two-dimensional parameter space to mimic the momentum in a two-dimensional lattice, it is more accurate to describe $\sqrt{\det g}$ as an area-form, but we maintain the more general terminology.

¹⁵We omit the calculation for brevity as it is not particularly illuminating.

model we are considering [17]. The Chern number can then be simply computed as [17]

$$\mathcal{C} = \frac{1}{2\pi} \int_{\text{MBZ}} d^2k \cdot \left(-\frac{1}{B} \right) = -\text{sgn}(B). \quad (41)$$

where MBZ denotes the magnetic Brillouin zone, with area proportional to the magnetic field strength. To recap, the Berry curvature is constant across all Landau levels, which implies that $\mathcal{C} = 1$ (for \mathbf{B} along $-\hat{z}$) for all Landau levels. All Landau levels are therefore topologically equivalent since they have the same Chern number. The geometric tensor however varies across Landau levels but is still momentum-independent, an immense simplification. Note that the inequality we derived earlier is saturated for the LLL. Also note that the magnetic field, and therefore the Chern number, inverses sign under time-reversal symmetry. This is a general property of the Chern number and implies that the model must break time-reversal symmetry to obtain non-trivial topology.

2.6 Quantized Hall conductivity from topology

Ultimately, we are interested in computing the Hall conductivity, which requires analyzing the response of the lattice model to an electric field perturbation. Consider the combined Hamiltonian $H = H_0 + H_1$ where H_0 is the original static Hamiltonian and H_1 is a time-dependent perturbation. We will refrain from explicitly defining the perturbation H_1 to keep the formalism general. In the Schrodinger picture, we have the time-dependent Schrodinger equation $i\partial_t |\psi(t)\rangle = H|\psi(t)\rangle$. Instead, the interaction picture is utilized where operators are time-evolved by H_0 , and states are time-evolved by H_1 , obtaining the equation

$$i\partial_t |\phi(t)\rangle = \tilde{H}_1(t) |\phi(t)\rangle, \quad \tilde{H}_1(t) = U_0^\dagger H_1(t) U_0 \quad (42)$$

where $|\phi(t)\rangle = U_0^\dagger |\psi(t)\rangle$ and $U_0 = \exp(-iH_0 t/\hbar)$. We assume that $\phi_0 \equiv \phi(-\infty) = \psi(-\infty)$ is an eigenstate of the combined Hamiltonian $H(t = -\infty)$. In this picture, we can write the first-order approximation to the state [14, 7]

$$\begin{aligned} |\phi(t)\rangle &\approx |\phi_0\rangle + \int_{-\infty}^t dt' \cdot \partial_{t'} |\phi(t')\rangle \\ &= |\phi_0\rangle - \frac{i}{\hbar} \int_{-\infty}^t dt' \cdot \tilde{H}_1(t') |\phi(t')\rangle \\ &= |\phi_0\rangle - \frac{i}{\hbar} \int_{-\infty}^t dt' \cdot \tilde{H}_1(t') U_0^\dagger U |\phi_0\rangle \\ &\approx |\phi_0\rangle - \frac{i}{\hbar} \int_{-\infty}^t dt' \cdot \tilde{H}_1(t') |\phi_0\rangle. \end{aligned} \quad (43)$$

We developed this formalism in order to evaluate expectation values in a first-order approximation. Substituting the result for the state, we obtain the expression

$$\begin{aligned} \langle A(t) \rangle_{\psi(t)} &= \langle \tilde{A}(t) \rangle_{\phi(t)} \\ &= \langle \tilde{A}(t) \rangle_0 + \frac{i}{\hbar} \int_0^t dt' \cdot \left\langle [\tilde{H}_1(t'), \tilde{A}(t)] \right\rangle_0 \end{aligned} \quad (44)$$

where $\langle A \rangle_0 = \langle \phi_0 | A | \phi_0 \rangle$ and $\langle A \rangle_{\gamma(t)} = \langle \gamma(t) | A | \gamma(t) \rangle$. This expression is first-order in the interaction H_1 .

We assume a spatially uniform vector potential of the form $A_j(t) = A_{0,j}e^{-i\omega t}$, which implies the electric field $E_j(t) = -\partial_t A_j(t) = i\omega A_{0,j}e^{-i\omega t} \equiv E_{0,j}e^{-i\omega t}$, and so $E_{0,j} = i\omega A_{0,j}$. Note that we fixed the gauge so that the scalar potential vanishes, $A_0 = 0$. Since we are dealing with a spatially uniform field, the perturbation becomes $H_1 = -\text{vol} \cdot j^\mu A_\mu$ where $\text{vol} = \int d^3x$ is the volume of the system. Ultimately, we are interested in the DC Hall conductivity, but the equations are easier to solve in the more general AC case. We can then compute the expectation value of the current density [22]

$$\begin{aligned}\langle j_i(t) \rangle_{\psi(t)} &= \langle \tilde{j}_i(t) \rangle_{\phi(t)} \\ &= \langle \tilde{j}_i(t) \rangle_0 + \frac{i}{\hbar} \int_{-\infty}^t dt' \cdot \langle [\tilde{H}_1, \tilde{j}_i(t')] \rangle_0 \\ &= \frac{\text{vol}}{\hbar} \int_0^\infty dt' \cdot E^{0j} e^{-i\omega t'} \cdot \langle [j_j, \tilde{j}_i(t')] \rangle_0\end{aligned}\tag{45}$$

where in the last line, we assumed that the current in the absence of an electric field (the first term) vanishes, and we used time-translation symmetry (energy conservation) to shift the times. We now define the conductivity tensor $\sigma_{ij}(\omega)$ via the expression $\langle j_i(t) \rangle_{\psi(t)} \equiv \sigma_{ij}(\omega)E_{0j}$, and so we obtain the **Kubo formula** [22]

$$\sigma_{xy}(\omega) = \frac{\text{vol}}{\hbar\omega} \int_{\mathbb{R}_{\geq 0}} dt \cdot e^{i\omega t} \langle 0 | [j_y, \tilde{j}_x(t)] | 0 \rangle\tag{46}$$

where we use the integral domain notation, $\mathbb{R}_{\geq 0}$. To proceed, we expand the commutator, and substitute for the interaction-picture operators ($\tilde{A} = U_0^\dagger A U_0$) to obtain [22]

$$\begin{aligned}\sigma_{xy}(\omega) &= \frac{\text{vol}}{\hbar\omega} \int_{\mathbb{R}_{\geq 0}} dt \cdot e^{i\omega t} \sum_n \left(\langle 0 | j_y | n \rangle \langle n | j_x | 0 \rangle \cdot e^{i(\varepsilon_n - \varepsilon_0)t/\hbar} - \langle 0 | j_x | n \rangle \langle n | j_y | 0 \rangle \cdot e^{i(\varepsilon_0 - \varepsilon_n)t/\hbar} \right) \\ &= -\frac{i\text{vol}}{\omega} \sum_{n \neq 0} \left(\frac{\langle 0 | j_y | n \rangle \langle n | j_x | 0 \rangle}{\hbar\omega + \varepsilon_n - \varepsilon_0} - \frac{\langle 0 | j_x | n \rangle \langle n | j_y | 0 \rangle}{\hbar\omega + \varepsilon_0 - \varepsilon_n} \right),\end{aligned}\tag{47}$$

and we take the DC limit ($\omega = 0$) to obtain¹⁶

$$\sigma_{xy} \equiv \sigma_{xy}(\omega = 0) = i\hbar \cdot \text{vol} \sum_{n \neq 0} \frac{\langle 0 | j_y | n \rangle \langle n | 0 \rangle - \langle 0 | j_x | n \rangle \langle n | j_y | 0 \rangle}{(\varepsilon_n - \varepsilon_0)^2}.\tag{48}$$

The rigorous derivation for the Kubo formula involves solving with general temperature $T \neq 0$, and then taking the DC limit $\omega = 0$ before taking the zero temperature limit. We utilized the opposite sequence of limits, but luckily these limits commute, and so we obtained the same result. To see the finite temperature calculation, which is significantly more challenging, see [2]. It seems a bit mysterious that the conductivity should involve terms in all bands, even unoccupied bands, when we know that conduction bands do not contribute to conductivity since the system is a bulk-insulator. This technicality will be resolved once we simply the Kubo formula, and these contributions seemingly disappear.

¹⁶Taylor expand the reciprocal of the denominators to first order in ω , and the $\mathcal{O}(1)$ term can be discarded due to gauge invariance. See [22].

To obtain a more useful formula, we express the current density operators as proportional to the group velocity, $j_j = e/\hbar \cdot \partial_\mu \tilde{H}$. Also note that $\langle m | \partial_\mu n \rangle = \langle m | \partial_\mu \tilde{H} | n \rangle / (\varepsilon_n - \varepsilon_m)$ ¹⁷, which we combine with the expression for the current density operator to achieve the **TKNN invariant**¹⁸ [22]

$$\sigma_{xy} = \frac{e^2}{h} \sum_\alpha \mathcal{C}_\alpha \quad (49)$$

where $\mathcal{C}_\alpha \in \mathbb{Z}$ is the Chern number of the occupied band α . Each occupied band α contributes $\sigma_{xy}^\alpha \equiv e^2 \mathcal{C}_\alpha / h$ to the Hall conductivity. Only the occupied bands contribute to the Hall conductivity. In the present formalism, we assumed periodic boundary conditions in deriving the TKNN invariant, and it is a bulk quantity since it involves the Chern numbers, which are integrals over the BZ. While the Berry curvature also contributes to the longitudinal component of the conductivity σ_{ii} , it is a non-topological term (not quantized). In addition, the AC Hall conductivity is also not quantized.

2.7 Quantized Hall conductivity in Landau levels

Each Landau level has Chern number $\mathcal{C} = 1$, and therefore contributes $\sigma_{xy} = e^2/h$ to the Hall conductance. Miraculously, the Hall conductance is quantized. Note that the Chern number is a bulk quantity, and measures the bulk Hall conductance. After all, we assumed periodic boundary conditions to derive the Kubo formula, and therefore there is no boundary (edges).

Consider what happens when we place two materials with different Chern numbers, $\mathcal{C}_1 < \mathcal{C}_2$, adjacent to each other. Within each material, there is an insulating gap since each material is a bulk insulator. The topology of a material (represented by the Chern number) cannot change without the gap closing (a non-adiabatic process). Since the topology changes at the interface, the gap must also close, and therefore valence bands from the \mathcal{C}_1 material must meet conduction bands of \mathcal{C}_2 . The valence bands must then cross the Fermi level, and the delocalized (topological) valence band becomes a so-called edge state, a delocalized state in the conduction band. The number of edge states is equal to the number of valence bands that cross the Fermi level, $\Delta\mathcal{C} \equiv \mathcal{C}_2 - \mathcal{C}_1$. Further, these edge states possess chirality (and are hence termed **chiral edge states**) since depending on the direction of the magnetic field and the orientation of the manifold, they all flow along a single direction. For instance, for a square, the edge states may flow in the clockwise or counter-clockwise directions.¹⁹

A material with a boundary (and Chern number \mathcal{C}) can be viewed as two materials, where the second material is simply the vacuum and has trivial Chern number. Therefore, we expect $\Delta\mathcal{C} = \mathcal{C}$ edge states at the boundary of the material. These topological considerations must be taken into account to conclude that Landau levels possess chiral edge states. The existence of edge-states is truly a topological result. Without the bulk, there is no boundary.²⁰ This deep connection between the bulk and edge is known as the **bulk-edge (or bulk-boundary) correspondence**.

To understand the origin of the finite width of Hall plateaux, we have to consider the role of disorder in the system. The sample is not perfect as there are impurities that localize electrons in the bulk. As the filling factor (the ratio of the band that is filled) ν is increased starting from $\nu = 0$, these

¹⁷See eqn. 104 for a proof.

¹⁸The integral over the BZ to obtain the Chern numbers appears as a generalization of the volume factor.

¹⁹Note that we have not yet introduced the electric field into the picture. Without the electric field, the edge states balance out and there is no net current.

²⁰An independent theory of quantized Hall transport cannot exist on a one-dimensional boundary in the absence of a bulk. Such attempts immediately run into issues such as the chiral anomaly where charge is not conserved.

localized states are filled first. Since the edge states have relatively high energy, they will not be filled until the localized bulk states have been filled. In the absence of disorder, all of the states in the bulk have the same energy, and so the chemical potential is precisely at the Landau level energy. Therefore, while the edge states of the bands below charge-neutrality are contributing to Hall transport, there are a macroscopic number of localized bulk states that must be filled before the edge states of the next band can contribute to Hall transport. As the magnetic field is increased, the magnetic length decreases, and the Landau level degeneracy increases. Therefore, filling the Landau level requires more electrons, and thus the width of the Hall plateaux is increased at larger magnetic field. As the magnetic field is tuned to zero, the Hall plateaux width also approaches zero, and the Hall conductivity assumes the inverse-linear contribution from the bulk, $\sigma_{xy} = n_{eq}/B$. With fixed doping (number of electrons), if the magnetic field is increased then since the Landau level energy spacing increases, and the Landau level degeneracy increases, electrons are shifted from the higher levels to the lower levels. In other words, higher magnetic fields correspond with lower filling fraction ν . Continuous changes in the magnetic field (or filling fraction) do not alter which is the highest Landau level (and therefore the Hall conductivity). These experimental knobs must be sufficiently altered in order to see a phase transition to a higher Landau level with qualitatively different effects.

3 Chern Insulator

The lattice was completely disregarded in the previous section since the magnetic length was significantly larger than the lattice spacing, and lattice effects, including considerations of symmetries became insignificant. In the IQHE, it is evident that the magnetic field plays the most important role in the manifestation of the effect. The magnetic field eliminates the Fermi surface in place of discrete-energy Landau levels. It seems almost mysterious that so much physics is derived from considering the simple model of a magnetic field perpendicular to a plane, and somehow we arrive at topological order.

One of the key points of the magnetic field is that it breaks time-reversal symmetry. To get an intuition for time-reversal symmetry, we consider a few examples. Momentum and angular momentum flip sign under time-reversal symmetry, and are therefore do not obey the symmetry. This is intuitive since if we reverse the direction of time, we see that the momentum also reverses, $p \equiv m \frac{dx}{dt} \mapsto m \frac{dx}{d(-t)} = -m \frac{dx}{dt} = -p$. On the other hand, the position and energy are time-reversal symmetric. The magnetic field, since it is generated by an electric current, does not obey time-reversal symmetry, and therefore the quantum Hall system as a whole does not obey this symmetry. This is most apparent when you consider the edge states which have a chirality to them. The edge states along the boundary of the manifold we are considering only flow along one direction due to simple considerations of the confinement potential and its orientation with respect to the bulk. Time-reversal reverses the sign of the magnetic field, and although the Landau levels are intact with the same magnetic length, the (chiral) edge states also reverse direction. It is clear that in order to manifest the IQHE, a basic requirement is that time-reversal symmetry is broken.

There is also a more general understanding of topological order. This formalism, which requires the introduction of quantum geometry and topology, will then allow us to reintroduce the lattice and consider whether the lattice itself can manifest the IQHE in the absence of a magnetic field, called the Integer Quantum Anomalous Hall Effect (IQAHE), or the **Chern insulator**.

3.1 Hofstadter bands

Before we attempt to study the lattice on its own (without a magnetic field applied), it is informative to consider the complete system of a magnetic field applied to a lattice with no approximations applied. This section is more for the interested reader and is less relevant to direct considerations of theorizing the Chern insulator. We follow the derivation provided in the seminal paper [8].

The most natural approach to introducing a lattice to the quantum Hall effect is to apply minimal coupling to the tight-binding model, instead of the free-particle Hamiltonian. Consider a square lattice with lattice constant a . There is a single energy band (since there is only one orbital) and the dispersion relation can be obtained

$$\varepsilon(\mathbf{k}) = \varepsilon_0(\cos k_x a + \cos k_y a) = \frac{\varepsilon_0}{2} \left(e^{ik_x a} + e^{-ik_x a} + e^{ik_y a} + e^{-ik_y a} \right) \quad (50)$$

which is just the two-dimensional generalization of the one-dimensional electron chain we considered earlier. We now introduce a magnetic field $\mathbf{B} = B\hat{z}$ perpendicular to the lattice and choose the Landau gauge $\mathbf{A} = Bx\hat{y}$. The exponentials in the energy dispersion can be interpreted as magnetic translation operators²¹ after applying minimal coupling $\hbar\mathbf{k} \mapsto \mathbf{p} - q\mathbf{A}$ to achieve $\varepsilon((\mathbf{p} - q\mathbf{A})/\hbar)$. For instance, we have

$$\psi(x_\mu + a) \equiv e^{ik_\mu a} \psi(x_\mu) \mapsto e^{i(p_\mu - qA_\mu)/\hbar} \psi(x_\mu) \quad (51)$$

which translates the wave function but also adds a phase factor due to the Aharonov-Bohm effect. In the Landau gauge, only the y -terms involve an induced phase, and the x -terms are the usual translation operators. We therefore have the time-independent energy equation

$$\varepsilon\psi(x, y) = \frac{\varepsilon_0}{2} \left(\psi(x + a, y) + \psi(x - a, y) + \psi(x, y + a)e^{-iqBxa/\hbar} + \psi(x, y - a)e^{iqBxa/\hbar} \right) \quad (52)$$

and we are interested in finding solutions to the energy ε . Note that the electron can only hop between square lattice sites, and so we discretize $x = na, y = ma$ for $n, m \in \mathbb{Z}$. Note that the phases depend only on x and so we are justified to assume plane-wave behavior in the y -component.²² The ansatz $\psi(x, y) = g(n)e^{i\nu m}$ where $g(n)$ is some function and, and ν depends on the energy. Using this ansatz, we obtain the reduced equation known as the Harper equation

$$g_{n+1} + g_{n-1} + 2\cos(2\pi n\alpha - \nu)g_n = \epsilon g_n \quad (53)$$

where $\epsilon = 2\varepsilon/\varepsilon_0$ and $\alpha = \phi(B)/\phi_0$ is the flux ratio where $\phi(B) = Ba^2$ is the magnetic flux penetrating a single lattice cell and $\phi_0 = \hbar/q$ is the flux quantum. We can rewrite the flux ratio as $\alpha = (a/l)^2/(2\pi)$ where $l = \sqrt{\hbar/qB}$ is the magnetic length. With fixed lattice constant, the parameter is the magnetic field strength, and we are interested in the resulting set of energy solutions $\epsilon_\alpha = \{\epsilon\}$ dependent on the magnetic field.

We are interested in the parameter ranges $\alpha \in [0, 1)$ since it can be shown that the spectrum satisfies $\varepsilon_{\alpha+N} = \varepsilon_\alpha$ for any $N \in \mathbb{Z}, \nu \in [0, 2\pi)$ since ν is a phase factor, and some straight-forward calculations shows that $\varepsilon \in [-4, 4]$. For $\alpha = 1$, assuming $a \approx 2\text{\AA}$ (roughly that of graphene), we require a magnetic field on the order of 10^9G and so this is not physically realistic. However, we can create a much larger lattice spacing using two-layer materials such as TBG.

²¹Recall that translation operators are slightly modified (magnetic translation operators) to correct for the Aharonov-Bohm phase induced by the magnetic field.

²²More formally, $[H, p_y] = 0$ and so a basis can be found such that the eigenstates of the Hamiltonian are that of p_y , which are plane-waves in y .

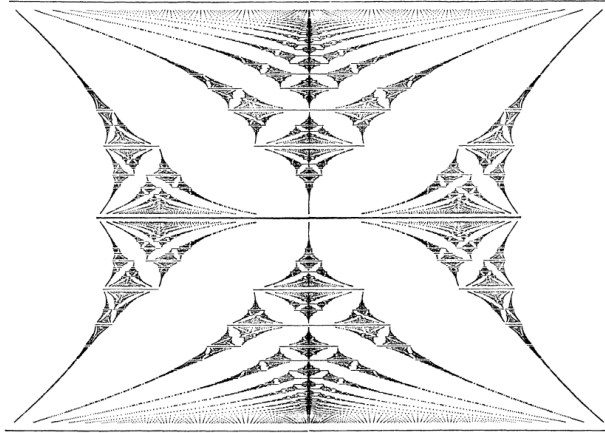


Figure 3: The fractal spectrum of Hofstadter bands. The horizontal axis is the energy $\varepsilon \in [-4, 4]$, and the vertical axis is the flux ratio α .

Note that for $\alpha = p/q$ (p, q coprime), referring to p/q flux quantum per unit cell, the Bloch band breaks up into q distinct energy bands (physically, the BZ has shrunk by a factor of q since the unit cell has increased in size by a factor of q to maintain periodicity and have an integer number (p) of flux quanta per unit cell). For magnetic translation operators to commute, the parallelogram they define must enclose $\mathbb{Z}\phi_0$, and the primitive unit cell becomes the ϕ_0 unit cell since it is the smallest of such unit cells. Since we have chosen the Landau gauge, the x direction becomes trivial (since no phase is accrued while translating along x) while that y is nontrivial. We define the magnetic translation operator to translate by a in the x axis, and a/α (or $P = 1/\alpha$ lattice spacings) in the y direction so that in total the unit cell encloses ϕ_0 and the problem becomes 1-dimensional in some sense, as the Harper equation above suggests. Note that by construction, $P = 1/\alpha \in \mathbb{R}$ is generally not an integer, but this does not prevent us from properly defining the primitive unit cell.

For $\alpha \in \mathbb{R} - \mathbb{Q}$ (irrational), there are infinitely many energy bands since a unit cell cannot be properly defined (we cannot multiply the irrational α flux quantum in the square unit cell by an integer to yield an integer) and lattice site becomes an orbital index. It would seem that there is an issue since both the rationals and irrationals are dense in \mathbb{R} (any $x \in \mathbb{R}$ is arbitrarily close to both an irrational number and a rational number), and therefore the spectrum is discontinuous. This is not the case since the rational contributions to the spectrum flow continuously, bringing some order to the spectrum. The resulting energy spectrum is a fractal known as Hofstadter's butterfly and is a beautiful realization of the complexity of the complete system of a lattice and magnetic field.

Hofstader bands become relevant under very high magnetic fields where the lattice becomes relevant as the magnetic length is on the same scale to the lattice constant. Hofstader bands also have edge states. We are interested in a model without a magnetic field, but it is nonetheless interesting how the lattice fits into the picture and changes the spectrum.

3.2 Chern insulator models

We now have some physical intuition for the Chern number. The Chern number of an occupied band is proportional to the Hall conductivity that band contributes. Now let us return to the mathematical description and seek some intuition.

The most general form of a two-dimensional (momentum-space) lattice Hamiltonian can be expressed as [22]

$$H(\mathbf{k}) = \boldsymbol{\mu}(\mathbf{k}) \cdot \boldsymbol{\sigma} + \nu(\mathbf{k}) \cdot \mathbf{1} \quad (54)$$

where $\boldsymbol{\sigma} = (\sigma_1, \sigma_2, \sigma_3)$ is a vector of Pauli matrices, and $\mathbf{k} \in \text{BZ} \cong T^2$. The energies of this general model can then be solved, $\varepsilon(\mathbf{k}) = \nu(\mathbf{k}) \pm |\boldsymbol{\mu}(\mathbf{k})|$.²³ Defining the unit vector $\boldsymbol{\eta}(\mathbf{k}) \equiv \boldsymbol{\mu}(\mathbf{k})/|\boldsymbol{\mu}(\mathbf{k})| \in S^2$, we can compute the Chern number [22]

$$\mathcal{C} = \frac{1}{4\pi} \int_{\text{BZ}} d^2k \cdot \boldsymbol{\eta} \cdot (\partial_x \boldsymbol{\eta} \times \partial_y \boldsymbol{\eta}) \quad (55)$$

where the derivative term $(\partial_x \boldsymbol{\eta} \times \partial_y \boldsymbol{\eta})$ is the area measure, and the dot product with $\boldsymbol{\eta}$ measures the area of the unit sphere (with sign) swept out as we vary \mathbf{k} over the BZ. In other words, \mathcal{C} counts how many times the map $\text{BZ} \cong T^2 \rightarrow S^2$ fully covers the origin, which is manifestly a topological invariant.

Now that we understand the mathematical description of the Chern number, at least for lattice models, let us consider a lattice model with non-zero Chern number. Most literature reviews will demonstrate the existence of a lattice model with non-trivial topology (non-zero Chern number) by deriving an analyzing the first model, the Haldane model built on graphene, a honeycomb lattice. To emphasize that graphene is not particularly special, we instead consider the checkerboard lattice model, a square lattice with two sublattices. Topologically, the two models are equivalent (they have the same Chern numbers), but their geometry is distinct.

We focus our attention on the checkerboard lattice and later return to Haldane's model. The checkerboard lattice is a square lattice comprised of two sublattices which enables an orbital degree of freedom, $\alpha \in \{A, B\}$. The importance of two-band model is paramount. A single-band model cannot have non-trivial Chern number since the sum of the Chern number of all bands must vanish (we will prove this later). Consequently, the two-band model is the simplest model in which a non-trivial Chern number can manifest.

The tight-binding Hamiltonian for this checkerboard model can be written [21]

$$H = -t \sum_{\langle i,j \rangle} e^{i\phi_{ij}} (c_i^\dagger c_j + h.c.) - \sum_{\langle\langle i,j \rangle\rangle} t'_{ij} (c_i^\dagger c_j + h.c.) - t'' \sum_{\langle\langle\langle i,j \rangle\rangle\rangle} (c_i^\dagger c_j + h.c.) \quad (56)$$

where the terms correspond to nearest-neighbor (NN), next-nearest-neighbor (NNN), and next-next-nearest-neighbor (NNNN) respectively.²⁴ There are four parameters in this model, including the NN hopping strength t and the associated phase $\phi_{ij} = \pm\phi$, the NNN hopping strength $t'_{ij} = \pm t'$, and the NNNN hopping strength t'' (independent of sublattice hopping). The NN phase and NNN hopping strength are dependent on the direction of sublattice hopping and are indicated in the figure.

The NN complex hoppings, $e^{i\phi_{ij}}$, depart from the real-valued hoppings we used to define the tight-binding model of the one-dimensional chain. However, there is no reason why complex hoppings should be deemed unphysical. As long as the Hamiltonian is Hermitian, there is no problem in theory. In fact, complex terms are necessary since we must break time-reversal symmetry, which is an anti-unitary operation, meaning that it involves taking the complex-conjugate. Therefore, to

²³An insulator phase can (and will) only occur given that $|\boldsymbol{\mu}(\mathbf{k})| \neq 0$ for all \mathbf{k} .

²⁴The Haldane model only includes NN and NNN terms, with the latter complex and the former real. Therefore the Haldane model is simpler to write down, but we consider this model for principle.

break time-reversal symmetry, the parameters we use must not be their own complex-conjugates. The complex hopping resembles the Aharonov-Bohm phase induced by a magnetic field. However, since the electrons are localized on the lattice (assumption of the tight-binding model), we have a discrete analogue of the Aharonov-Bohm phase. In addition, this phase is not the result of an external magnetic field but is an intrinsic property of the lattice. Therefore, it would not be totally surprising that we would get a lattice-analogue of the IQHE.

We perform a Fourier transform to obtain the momentum-space representation, [21]

$$H = ((t'_1 + t'_2)(\cos k_x + \cos k_y) + 4t'' \cos(k_x) \cos(k_y)) \cdot \mathbf{1} + 4t \cos \phi \cos \frac{k_x}{2} \cos \frac{k_y}{2} \cdot \sigma_x + 4t \sin \phi \sin \frac{k_x}{2} \sin \frac{k_y}{2} \cdot \sigma_y + (t'_1 - t'_2)(\cos k_x - \cos k_y) \cdot \sigma_z, \quad (57)$$

which is rather unruly. Time-reversal symmetry is preserved at $\phi = n\pi$ for $n \in \mathbb{Z}$, so we must avoid those parameters to obtain non-trivial topology. For parameter values $\phi = \pi/4$, $t = 1$, $t'_1 = -t'_2 = 1/(2 + \sqrt{2})$, $t'' = 1/(2 + \sqrt{2})$, the bands carry Chern number ± 1 .

Note that while the bands are topologically non-trivial similar to Landau levels, the geometry of the two models are distinct. As mentioned before, the QGT (and the band-structure) of Landau levels (and therefore all geometric quantities) is independent of momentum, unlike the QGT of of checkerboard lattice. It is known that lattice models cannot exactly replicate the geometry of the LLL [24].

As mentioned, a more simple model would be the Haldane model built on the graphene honeycomb lattice, [7]

$$H = -t_1 \sum_{\langle iA, jB \rangle} (c_{iA}^\dagger c_{jB} + h.c.) + m \sum_i (n_{iA} - n_{iB}) - t_2 \sum_{\langle \langle i\alpha, j\alpha \rangle \rangle} (e^{i\Phi_\alpha} c_{i\alpha}^\dagger c_{j\alpha} + h.c.) \quad (58)$$

where the terms correspond to a NN hopping, an on-site potential, and a complex NNN hopping. Notably, the NNNN hopping is not necessary, unlike the checkerboard lattice. We perform a Fourier transform to obtain the momentum-space representation [7]

$$H(\mathbf{k}) = \begin{pmatrix} -2t_2\gamma_\Phi(\mathbf{k}) + m & -t_1f(\mathbf{k}) \\ -t_1\overline{f(\mathbf{k})} & -2t_2\gamma_{-\Phi}(\mathbf{k}) - m \end{pmatrix} \quad (59)$$

where $\gamma_\Phi(\mathbf{k}) = e^{i\Phi}(e^{-i\mathbf{k}\cdot\mathbf{a}_1} + e^{-i\mathbf{k}\cdot(\mathbf{a}_2-\mathbf{a}_1)} + e^{i\mathbf{k}\cdot\mathbf{a}_2})$, $f(\mathbf{k}) = \sum_{j=1}^3 e^{-i\mathbf{k}\cdot\boldsymbol{\tau}_j}$, \mathbf{a}_i are the primitive lattice vectors of graphene, and $\boldsymbol{\tau}_i$ are the NN (momentum-space) hopping vectors. For $|m| < |3\sqrt{3}t_2 \sin \Phi|$ and assuming $\Phi \neq n\pi$ (break time-reversal symmetry), the bands carry Chern number ± 1 .

4 Fractional Quantum Hall Effect

It seems that Landau level physics and the IQHE, and its lattice analogue are completely solved. The IQHE was first discovered experimentally in GaAs heterostructures and then explained theoretically in terms of the bulk Chern number and accompanying edge states in the presence of a boundary. Lattice analogues of the IQHE manifest in the case that the topology of the lattice band matches that of the Landau level, with Chern number $\mathcal{C} = 1$. For higher Chern numbers in the case of the lattice, we simply have more edge states per occupied band. Landau level physics and the IQHE have been completely discussed and analyzed in terms of non-interacting physics. The Chern number only assumes knowledge of the single-particle Bloch states, and the Landau level

Hamiltonian neglects interactions. A priori, there is nothing wrong with this assumption. Single-particle effects dominate if the interaction is relative weak. That is, if the interaction strength is much smaller than the band gap and the band-width, then the interaction is not at risk of exciting states between bands or dominating over the kinetic energy, respectively.

Even more directly, if the Landau level, or any band, is completely filled, $\nu \in \mathbb{Z}$, then intra-band interactions are not relevant anyway, although states might still be scattered between bands. Therefore, we at least do not expect to see many-body physics at integer fillings. In general however, it should not be a surprise that we see many-body physics at fractional filling. The electrons interact via Coulomb repulsion, and this must be taken into consideration to fully consider the physics. Interacting effects at fractional filling are collectively termed the **fractional quantum Hall effect (FQHE)**. Although the names are similar, it is important to emphasize that the origin of the IQHE and the FQHE are entirely distinct. The IQHE is a non-interacting effect while the FQHE is caused by interactions.

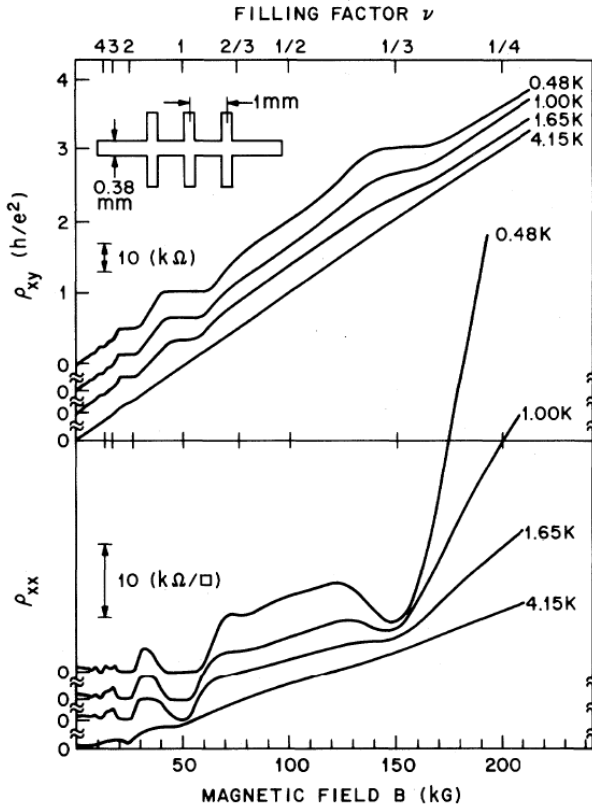


Figure 4: Hall and longitudinal resistivity as a function of magnetic field strength. The first Hall plateau at fractional filling factor $\nu = 1/3$ is experimentally measured by Tsui [23].

4.1 Interactions in flat band models

A priori, it is not clear which interaction could be responsible for the effects at fractional filling factor. When discussing the IQH effect, we did not consider spin (equivalently, we considered a spin-polarized system), and we did not consider inter-electron Coulomb interactions. We also did not consider the Zeeman effect coupling. After all, electrons have spin and we are subjecting them to a strong magnetic field. We will now discuss these interactions and show that the Coulomb

interaction is the crucial ingredient. Consider a system of N particles, with Hamiltonian [10]

$$H = \frac{1}{2m} \sum_{j=1}^N \mathbf{\Pi}_j^2 + \sum_{j=1}^N \sum_{k < j} \frac{e^2}{4\pi\epsilon_0 |\mathbf{x}_j - \mathbf{x}_k|} + g\mu_B \sum_{j=1}^N \mathbf{B} \cdot \mathbf{S}_j + \sum_{j=1}^N V_{disorder}(\mathbf{x}_j) \quad (60)$$

where the first term is the kinetic energy of an electron in a magnetic field (resulting in Landau levels), the second term is the Coulomb interaction between the electrons, the third term is the Zeeman effect, and the last term is the potential created by disorder. In strong magnetic fields, the Zeeman effect dominates over the Coulomb interaction, and we expect the electrons to be spin-polarized. Therefore we essentially treat $\mathbf{B} \cdot \mathbf{S}$ as a constant and drop it from the Hamiltonian. We do not consider the effect of the disorder potential because as in the treatment of the IQH effect, disorder is not relevant to the essential physics, but is the source of the finite width of the Hall plateaux. In other words we first develop the physics in the absence of disorder, and then invoke it afterwards when discussing the plateaux. The only terms that remain are the kinetic energy and Coulomb interaction

$$H = \frac{1}{2m} \sum_{j=1}^N \mathbf{\Pi}_j^2 + \sum_{j=1}^N \sum_{k < j} \frac{e^2}{4\pi\epsilon_0 |\mathbf{x}_j - \mathbf{x}_k|}. \quad (61)$$

The kinetic energy term is responsible for forming Landau levels. Once we have Landau levels, the only interaction, or the only perturbation, is the Coulomb interaction. This is the source of difficulty in solving the FQHE. There is effectively only a single term present in the Hamiltonian, the Coulomb interaction. Perturbation theory is rooted in comparing two terms, a known, exactly-solvable base term, and a perturbation whose solution is difficult to derive analytically. The unsolvable term is then expanded as a perturbative series to simplify the interaction, relative to the base term. Since we do not have a base term, we cannot use terms from perturbation theory (including quantum field theory).

4.2 Laughlin states

All hope is not lost though. Given the form of the Coulomb interaction as a repulsive, central potential, Laughlin was able to provide an ansatz for the ground state wave function [12]. Recall that the LLL single-electron wave function in the symmetric gauge can be expressed as [7, 5]

$$\psi(z) = f(z) \cdot e^{-\frac{1}{4}|z|^2} \quad (62)$$

where $f(z)$ is a polynomial in the variable $z = x - iy$.²⁵ The N -electron wave function can be constructed by taking the Slater determinant of the single-particle wave function to obtain²⁶

$$\psi[z] = f[z] \cdot e^{-\frac{1}{4} \sum_{i=1}^N |z_i|^2} \quad (63)$$

where

$$f[z] \equiv \begin{vmatrix} z_1^0 & \dots & z_N^0 \\ \vdots & . & \vdots \\ z_1^{N-1} & \dots & z_N^{N-1} \end{vmatrix} = \prod_{i < j}^N (z_i - z_j). \quad (64)$$

²⁵Note that $\psi(z)$ itself is not a holomorphic function since the exponential term depends on \bar{z} ($|z|^2 = z\bar{z}$)

²⁶This wave function is only equal to the actual wave function up to some irrelevant constants.

The Slater determinant is used to construct an anti-symmetrization of a product-state wave function. This anti-symmetrization is required for the many-body wave function to satisfy fermionic anti-commutation relations. In our case, each orbital corresponds to an angular momentum value m , which is simply the power of z_i . We use the notation $[z] = (z_1, \dots, z_N)$ to denote the positions of the N particles. It is clear that the wave function is antisymmetric under particle exchange as is required for a system of fermions. In other words, $f[z] \mapsto -f[z]$ under the exchange of particle coordinates $z_i \leftrightarrow z_j$ ($i \neq j$). In addition, $f[z]$ is a homogenous polynomial in the variable z_i , and the highest power of any z_i that appears is $N - 1$. Consequently the state $\psi[z]$ corresponds to the case where all the states from $m = 0$ to $m = N - 1$ are occupied, and therefore the filling factor is $\nu = 1$. By fully filling the LLL, we have constructed the N -electron wave function without considering the Coulomb interaction at all as is the case for the IQHE. It turns out that this wave function is the unique state of any two-body interaction potential in the LLL which both maximizes the electron density and minimizes the total angular momentum (due to the Gaussian factor), which we will shortly derive using Haldane pseudopotentials.

The physical meaning behind the Slater determinant term is to push electrons away from each other. With fixed particle configuration $[z]$, the wave function amplitude $|\psi[z]|^2$ provides the probability density of such a configuration. This is analogous to the single-particle case in which the amplitude $|\psi(z)|$ gives the probability density of the particle residing at position z . Consider the case where two particles are near each other $z_i \approx z_j$. Then the factor that includes these particle indices would minimize the wave function, $z_i - z_j \approx 0$, and therefore $|\psi[z]|^2 \approx 0$. The Slater determinant term therefore does not allow two electrons to occupy the same position $z_i = z_j$ since it assigns zero probability density to that configuration. More generally, the term assigns a lower probability density to configurations in which electrons are closer to each other. Physically, this is motivated by the fact that the Coulomb interaction pushes electrons away from each other, and therefore one would not expect to see electrons close to each other.

We now consider the case of a partially-filled LLL, $\nu < 1$. Laughlin postulated the so-called **Laughlin state** ansatz [12]

$$\psi[z] = f[z] \cdot e^{-\frac{1}{4} \sum_{i=1}^N |z_i|^2}, \quad f[z] = \prod_{i < j} f(z_i - z_j) \quad (65)$$

and then restricted the form of $f(z)$ due to first-principles considerations. As before $\psi(z)$ must be antisymmetric upon particle exchange and therefore $f(z)$ must be odd. Due to conservation of angular momentum, we require that $f[z]$ is a homogenous polynomial of degree M where M is the total angular momentum. This restricts the form to $f(z) = z^m$ for some odd positive integer m , and thus we have

$$f[z] = f_m[z] \equiv \prod_{i < j}^N (z_i - z_j)^m \quad (66)$$

and denote the corresponding wave function by $\psi_m[z]$. $\psi_m[z]$ is the (approximate) eigenstate of the $\nu = 1/m$ filling factor. Note that each electron coordinate z_i has maximum degree $M = m(N - 1)$ which represents the maximum angular momentum that the electron may possess. Also note that $f_m[z]$ is the eigenstate of the operators $L_z^{ij} = \hbar((z_i - z_j)\partial_{ij} - \overline{(z_i - z_j)}\partial_{ij})$ where $\partial_{ij} = \partial/\partial(z_i - z_j)$, which measure the relative angular momentum between particles i and j .

4.3 Haldane pseudopotential

We are now ready to understand why the Laughlin state is the (approximate) ground state of $\nu = 1/m$. Of course, it is not the exact ground state since we projected the dynamics onto the LLL, thereby neglecting Landau level mixing, a justifiable approximation assuming that the Coulomb interaction strength is much less than the band gap to the next Landau level. Since the Laughlin state is not the (exact) ground state of the Coulomb interaction Hamiltonian, the natural question arises of whether it is the exact ground state of any Hamiltonian. Finding this Hamiltonian is important since it reveals the effective Hamiltonian in the LLL projection. Suppose that the angular momentum eigenstates $|Mm\rangle \approx (z_1 + z_2)^M \cdot (z_1 - z_2)^m$ are the eigenstates of the potential energy operator \hat{V} and we neglect writing the exponential factor for ease of notation. We are only considering a two-particle system, and therefore we only have indices 1, 2. Also note that the Hamiltonian simply becomes $H = \hat{V}$ since there is no kinetic energy in the LLL. Assuming the aforementioned eigenstates are normalized, we can easily express the eigenvalues of the potential $v_m \equiv \langle Mm | \hat{V} | Mm \rangle$, so-called **Haldane pseudopotentials** [7]. The eigenvalues v_m are independent of the total angular momentum M if we assume that V is a central potential.

As we derived earlier, the eigenstates $|Mm\rangle$ are rings with (approximate) radius $r_m = \sqrt{2ml_B}$, and so we can approximate the pseudopotentials $v_m \approx V(r = r_m)$ since contributions to the inner product (integral) are concentrated around the ring. Since r_m is discrete, we have that the pseudopotentials v_m are discrete. This is a strange result given that it is true irrespective of the sign of the potential, meaning that even for repulsive potentials, we have a discrete spectrum which is indicative of bound states. To recap, for a repulsive position, the two particles are necessarily a bound state. This strange behavior is due solely to the magnetic field. Without the magnetic field, quantum mechanics tells us that a repulsive potential only admits scattering (delocalized) states.²⁷ We can construct the effective Hamiltonian

$$H = \sum_{m=1}^{\infty} v_m P_m \tag{67}$$

where P_m is the projector onto the subspace with relative angular momentum m (and any M). Now consider the particular pseudopotential $v_{m'} = \mathbf{1}_{m' < m}$ which increases energy if the state has angular momentum below the fixed constant m . This pseudopotential is rather intuitive since lower angular momentum implies higher density near the origin, and thus the particles are closer to each other, and the Coulomb repulsion increases the energy. However, instead of having a gradual increase of energy for lower angular momentum, in this simple case, the interaction is only present below relative angular momentum m . For systems of many particles, there is a simple generalization $H = \sum_{m=1}^{\infty} \sum_{i < j} v_m P_m^{ij}$ where P_m^{ij} projects onto the subspace where particles i, j have relative angular momentum m . Considering the same pseudopotential as before, note that we can avoid the energy cost of low angular momentum (below m) by requiring that each pair of particles has angular momentum m , so we have the ansatz

$$\psi[z] = s[z] \cdot \prod_{i < j} (z_i - z_j)^m \tag{68}$$

where once again, we neglect writing the exponential factor. This ansatz is remarkably close to the Laughlin state ansatz in the previous section, and is exact if we assume the ambiguous factor

²⁷For instance, consider the free-particle Hamiltonian $H = \hbar^2 k^2 / 2m$ which gives us the spectrum $k^2 / 2m$ with k a continuous parameter and delocalized eigenstates $|k\rangle$ (definite momentum implies indefinite position).

vanishes, $s[z] = 1$. To intuitively understand where this condition comes from, note that we have thus far omitted the confining potential of the sample in our considerations. With $s[z] = 1$ the Laughlin state corresponds to the most compact (high electron density) state while maintaining minimum relative angular momentum m . Therefore, the Laughlin state is the most optimized state in this regard, where we assume that the confining potential is weaker than the energy gap to the next lowest angular momentum, $m - 1$. To write the effective Hamiltonian, considering the confining potential, we note that states with lower electron density, or a larger radius have a higher angular momentum, and so we can write ωL_z in place of the confining potential.²⁸ The effective Hamiltonian becomes [7]

$$H = \sum_{m=1}^{\infty} \sum_{i < j} v_m P_m^{ij} + \omega L_z \quad (69)$$

where ω is some constant that is lower than the aforementioned energy gap. The first term of this Hamiltonian states that there is a finite energy to squeeze the wave function (increase the electron density) which leads us to the notion that the Laughlin state is an **incompressible quantum fluid**. In the more familiar case of water, it is also an incompressible fluid which means that it takes a significant amount of force in order to raise the density of water. For the Laughlin state, incompressibility implies a gap in the bulk spectrum since it costs a finite energy to lower the angular momentum (change eigenstates).

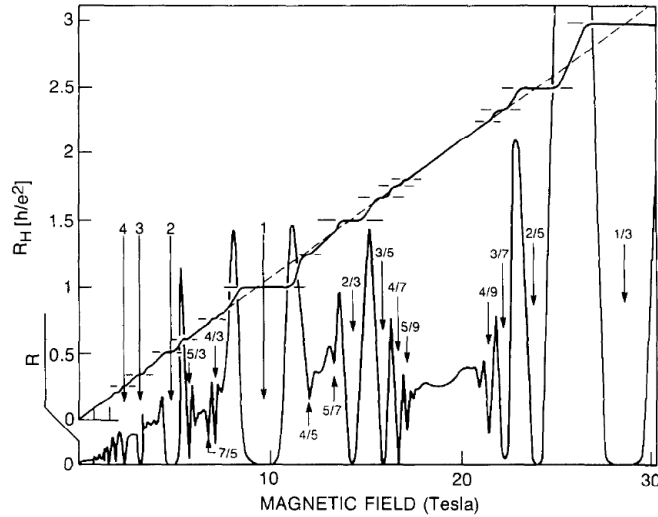


Figure 5: Hall and longitudinal resistivity as a function of magnetic field strength. Hall plateaux can be seen at numerous fractional filling factors as experimentally measured by Stormer [20].

4.4 Topological degeneracy of ground state manifold

We have thus far only discussed ground states of the $\nu = 1/m$ filling factor. It turns out that excited states, so-called quasiholes and quasiparticles, have exotic properties including fractional charge ($\pm 1/m$ respectively), and fractional anyonic statistic $\phi_m \equiv e^{2\pi i/m}$. As the names suggest, a quasihole is the removal of an electron from $\nu = 1/m$, and a quasielectron is the addition of an electron to $\nu = 1/m$. The anyonic statistic is a familiar quantity to us, as it quantifies the phase induced by exchanging particles. For instance, for fermions (e.g. electrons) and bosons (e.g.

²⁸This is convenient since we are working with angular momentum eigenstates.

photon) the anyonic statistic is ± 1 respectively. It is remarkable that a collection of fermions can give rise to an excitation with anyonic statistic ϕ_m . Particles that are neither fermions nor bosons are termed **anyons**. There are no fundamental particles which are anyons; they must be quasiparticles, and can only exist in two-dimensions as our earlier topological argument proved.

We will now explore how the anyonic statistics of Laughlin quasiholes and quasiparticles implies a degeneracy of the ground state manifold (GSM). Consider the pair-creation of a quasihole and quasiparticle from the vacuum, and the action of the translation operators T_x, T_y on these particles, which translates them around the BZ (torus) in the \hat{x}, \hat{y} direction respectively. One can convince themselves that the combined action $T_x T_y T_x^{-1} T_y^{-1}$ is equivalent to braiding the particles around each other, and therefore acquiring a phase as a result of the anyonic statistics. In the Laughlin $\nu = 1/m$ state, the phase amounts to $\phi_m \equiv e^{2\pi i/m}$. Note that we have the operator equality $T_x T_y T_x^{-1} T_y^{-1} = \phi_m \cdot \mathbf{1}$. In addition, we have the requirements $T_x^3 = T_y^3 = \mathbf{1}$ which amounts to wrapping a particle around a torus three times.²⁹ It is clear that $[T_x, T_y] \neq \mathbf{1}$, and so a representation of these operators would have to have greater than one dimension since scalars commute. It turns out that the unique irreducible representation of these operators has dimension m , and is defined by the action $T_x |n\rangle = \phi_m^n |n\rangle$, $T_y |n\rangle = |n+1\rangle$, $T_y |m\rangle = |1\rangle$ for an m -dimensional vector space V spanned by $\{|n\rangle\}_{n=1}^m$. Hence, the ground state manifold has m distinct, orthogonal states (with the same energy). In general, the number of ground states depends on the topology of the compact manifold we are considering. Since the BZ of a two-dimensional lattice is topologically equivalent to a torus, it was natural to consider a torus.³⁰

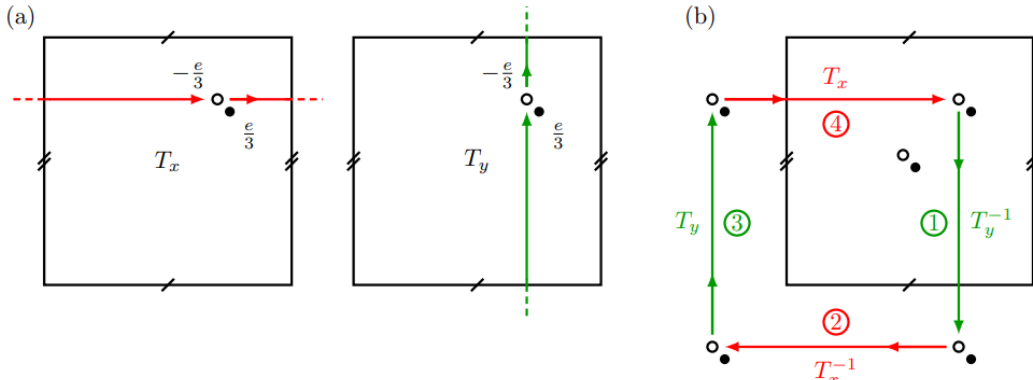


Figure 6: (a) Translations of a quasi-hole, quasiparticle pair along the \hat{x} and \hat{y} axes. (b) Combined translation, $T_x T_y T_x^{-1} T_y^{-1} = \phi_m \cdot \mathbf{1}$ [5].

The degeneracy of the GSM is a quantity we can easily measure from the many-body spectrum, but it need not be related to the manifestation of the FQH gap. Nonetheless, it is a necessary condition.

5 Fractional Chern Insulator

In the quantum Hall effect, a magnetic field is applied transverse to the planar sample. This magnetic field breaks time-reversal symmetry, and quantizes the energy levels of the electrons,

²⁹We need to wrap the particle around the torus three times to cancel out the phase that it acquires from the boundary conditions.

³⁰For a two-dimensional compact manifold with genus g (number of holes), the degeneracy generalizes to m^g .

called Landau levels. We will not directly utilize the technical details of the derivation of Landau levels, or the quantum Hall effect in general, and will instead speak of the effect in phenomenological terms. One crucial feature of Landau levels is that they are non-dispersive, meaning that they are constant with respect to crystal momentum, so-called flat-bands. In addition, these bands become topological in the sense that they carry non-zero Chern number, and also have uniform Berry curvature. As we saw before, breaking time-reversal symmetry is necessary for obtaining topological bands since time-reversal symmetry flips the sign of the Chern number. In exploring the Haldane model, we saw how a lattice model can host Chern bands in the absence of a (net) magnetic field through complex hopping terms, breaking time-reversal symmetry. When filled, Chern bands yield the anomalous integer quantum Hall effect, a bulk-insulator state that hosts quantized Hall conductivity through transport on the boundary. In deriving the Chern number and the integer quantum Hall effect, we did not at all pay attention to electron interaction terms, such as Coulomb repulsion, and thus these phases are a single-particle phenomena, although there is certainly a bulk-edge correspondence in which the bulk is necessary to produce edge states on the boundary. The lack of dependence on electron interactions is quite natural considering that the bands must be completely filled ($\nu \in \mathbb{Z}$) in order to exhibit either of these phases. In filled bands, since the Fermi level is in the valence-conduction gap, all the available electron states are occupied and the off-diagonal matrix elements provided by the interaction cannot manifest in the sample. We will briefly cover the main properties of the FQHE, without heeding to the technicalities or derivations.

If the band is fractionally filled, then interactions are able to play a role in the dynamics, and in the case of Landau levels, the fractional quantum Hall effect (FQHE) manifests which includes a vast amount of rich phenomena depending on the material and filling factor. This effect is a generalization of the integer quantum Hall effect to fractional filling factor, but it is crucial to note that the origin of this effect is in inter-electron interactions (specifically Coulomb repulsion which we will discuss shortly) and certain (not entirely known) properties of Landau levels. An undisputed property of Landau levels necessary for the FQHE is their lack of dispersion. In a flat band, the kinetic energy is independent of momentum³¹, and therefore the potential energy is the only term that contributes to dynamics. The system naturally wants to minimize the energy, and thus solely minimize the potential energy, and therefore the interaction plays a crucial role in the dynamics compared to that of dispersive bands.

Similar to the case of the IQHE, we could attempt to generalize the FQHE to lattice models, arriving at the **fractional Chern insulator (FCI)**. Unlike the IQHE, we require flat bands so that the interactions play the central role in determining the dynamics when fractionally filled.³² The bands do not have to be perfectly flat, so long as the kinetic energy is negligible compared to the interactions. We also require the bands to be topological (non-zero Chern number) which requires the breaking of time-reversal symmetry. Requirements on the distribution of Berry curvature within the BZ are disputed. Naturally (or perhaps naively), one may desire to replicate Landau levels and require uniform Berry curvature, restricting the geometry of the bands, however, it is not clear whether this condition is necessary. Fractional Chern insulator states were measured in graphene-based lattices, but a small magnetic field was applied solely to correct for non-uniformities

³¹It is important to understand this statement. From the perspective of classical mechanics, it seems absurd that energy could be independent of momentum. We are too-familiar with writing the energy-momentum relation, $\varepsilon = p^2/(2m)$ in which the energy depends quadratically on the momentum. In flat bands, the energy is independent of momentum.

³²Recall that the bands of the Haldane model were not flat, and the origin of the quantum anomalous Hall effect is solely in obtaining a non-zero Chern number, a result that depends on the topology of the band, but not its geometry.

in Berry curvature. While this experiment was a significant stepping stone in realizing fractional Chern insulators, more recent experiments have measured these phases in the complete absence of magnetic fields, where the phase is entirely intrinsic.

We will begin with recent experimental work on detecting FCI phases, and will numerically compute interactions in lattice models that result in FCIs to shed light on the role of geometry in these models. Although the fundamental physics of these effects is fascinating, there are also ambitious applications to topological quantum computing that may motivate these pursuits.

Moire materials are a class of multi-layer lattices which enable tunable topological flat bands. The layers are twisted with respect to one another, resulting in a change in the periodicity of the lattice, and the electron dynamics. Under an arbitrary angle, the lattice is not commensurate, and therefore not periodic. However, a discrete, infinite set of angles exist in which the resulting structure is periodic, and the real-space unit cell is significantly larger, resulting in a smaller BZ. Certain moire materials, such as magic-angle twisted bilayer graphene (MATBG) and twisted bilayer MoTe₂ (molybdenum ditelluride), host topological flat bands, making them promising candidates as fractional Chern insulators. Earlier, we briefly mentioned the candidacy of MATBG through experiment, but the non-uniformity of the Berry curvature requires the application of a magnetic field to correct. Recent experiments have focused on small-angle twisted transition metal dichalcogenide (TMD) homobilayers³³ which host a more honeycomb lattice, similar to twisted bilayer graphene. These materials host strong spin-orbit coupling which locks the spin to the valley degree of freedom. In addition, numerical computations have demonstrated that these materials include complex hopping terms, as we explored in the Haldane model, but are an intrinsic property and not the result of an external magnetic field inducing Aharnov-Bohm phases. This complex hopping, along with precise twist angles result in nearly flat topological³⁴ bands with nearly flat Berry curvature distributions. Transport measurements suggest the existence of fractional Chern insulator phases in these class of materials.

5.1 Geometric Stability Hypothesis

To understand what geometric conditions [17, 13] are required for the manifestation of the FCI phase, let us first review Landau level physics. We introduce a density-density interaction term (e.g. $U \sum_{\langle i,j \rangle} n_i n_j$) where $n_i = c_i^\dagger c_i$ counts the number of states in state i [18, 16]. This interaction has strength U , and similar to the case of the FQHE, in the regime of large energy gap $\hbar\omega$ (proportional to magnetic field) compared to interaction strength U , we can neglect the scattering (or mixing) of states between Landau levels, greatly reducing the size and complexity of the problem.³⁵ Therefore, we can focus our attention solely on the LLL, which is topologically equivalent to the higher Landau levels, although the quantum metric is slightly different. In effect, by ignoring all of the remaining bands, we are projecting the physics onto the LLL. The (projected) interaction scatters momentum states within the LLL.

We must therefore project the density (number) operators, $\rho_{\mathbf{k}} = c_{\mathbf{k}}^\dagger c_{\mathbf{k}}$ onto the LLL using the projection operator $P = \sum_m |0, m\rangle \langle 0, m|$ where m denotes angular momentum (we chose the symmetric gauge representation) [17]. The projected density operator then becomes $\bar{\rho}_m = P \rho_{\mathbf{k}}^\dagger \rho_{\mathbf{k}} P$ since the fermion operators transform as $c_{\mathbf{k}}^\dagger \mapsto P c_{\mathbf{k}}^\dagger$ and $c_{\mathbf{k}} \mapsto c_{\mathbf{k}} P$ since P is Hermitian, as is

³³Homobilayers are a class of bilayer materials where both layers are the same lattice.

³⁴Spontaneous time-reversal symmetry breaking due to ferromagnetic ordering induces an intrinsic magnetization of spins in TMDs.

³⁵We will perform this approximate rigorously for the lattice model in the next section.

required by a projection operator.

If we also assume that the band-width of the projected band is negligible compared with the interaction strength, we can ignore the single-particle Hamiltonian entirely (since it approximates to a constant which does not affect the dynamics). Although we are neglecting the single-particle Hamiltonian, the Landau level physics is still crucial through the projection operators. Since the Landau level is dispersionless, we are entirely justified in applying this simplification. The total projected Hamiltonian is then simply $H_{\text{LLL}} = \bar{U}$ where $\bar{\cdot}$ denotes projection onto the LLL. Within the formalism of the Haldane pseudopotential expansion, the projected interaction can be written as [17]

$$H_{\text{LLL}} = \frac{1}{2} \int_{\text{BZ}} \frac{d^2\mathbf{k}}{(2\pi)^2} \cdot v(q) \sum_{i \neq j} \bar{\rho}_{-\mathbf{q}}^i \bar{\rho}_{\mathbf{q}}^j \quad (70)$$

where $v(q)$ are the Haldane pseudopotential terms (assuming a central potential. It turns out that the projected density operators satisfy the so-called W_∞ algebra (also called the **GMP algebra**, an acronym for its discoverers) [6, 17]

$$[\bar{\rho}_{\mathbf{q}_1}, \bar{\rho}_{\mathbf{q}_2}] = 2i \sin\left(\frac{(\epsilon_{z\mu\nu}/B)q_1^\mu q_2^\nu}{2}\right) \exp\left(\frac{q_1^\mu q_2^\nu/B}{2}\right) \bar{\rho}_{\mathbf{q}_1+\mathbf{q}_2} \quad (71)$$

where ϵ is the Levi civita totally anti-symmetric tensor. This algebra appears highly non-trivial to the eye.³⁶ The GMP algebra is satisfied by both the single-particle projected density operators, and also their multi-particle counterparts, $\sum_i \bar{\rho}_{\mathbf{q}}^i$. It might seem a little strange that we are studying interaction terms but are focusing on the algebra of single-particle states, but it is entirely justified in considering that the form of interaction we are considering (analogous to the Coulomb interaction) is described by the scattering of single-particle momentum states. It might therefore seem natural to attempt to recreate this algebra in a lattice model and call it a day. A priori, we could try to take a step back and just require that the geometry of the lattice model must be identical to that of the LLL. This turns out to be unnecessary, and even violate some rather elementary considerations of condensed matter physics, which we will discuss in the next section. However, for the sake of understanding, we will discuss the motivation behind these unnecessary and excessively strong criteria. Instead of out-right claiming that the geometry must be the same, let us require that the GMP algebra must be reproduced in the lattice model. Assuming that the GMP algebra matches, then if we match the pseudopotentials in the two models, then we should intuitively arrive at the same effective Hamiltonian with the same projected density operator algebra.

Consider the projected density operators of the lattice model, $\bar{\rho}_{\mathbf{k}}$. We can expand the commutation relations in (small) momentum, and cite that assuming the Berry curvature is constant, the same form of the GMP algebra manifests up to order $\mathcal{O}(q^2)$ [17]. If we also include that the quantum metric is constant, then we reach order $\mathcal{O}(q^3)$ [17]. Fully recreating the GMP algebra requires that the quantum metric vanishes, which is not allowed due to geometric constraints. If we assume saturation of the so-called determinant condition we derived earlier, $|\Omega_{12}|^2/4 = \det g$ as well as constant Berry curvature, the projected density operators satisfy a generalized form of the GMP algebra [17]

$$[\bar{\rho}_{\mathbf{q}_1}, \bar{\rho}_{\mathbf{q}_2}] = 2i \sin\left(\frac{\Omega_{\mu\nu} q_1^\mu q_2^\nu}{2}\right) \exp(g_{\mu\nu} q_1^\mu q_2^\nu) \bar{\rho}_{\mathbf{q}_1+\mathbf{q}_2} \quad (72)$$

which if we equate each term to that of the GMP algebra, we obtain equality given that $\Omega_{\mu\nu} =$

³⁶It is not particularly enlightening to derive this algebra.

$\epsilon_{\mu\nu}/B$, and $g_{\mu\nu} = 1/(2B) \cdot \delta_{\mu\nu}$. Therefore, these conditions on the geometry give us a sense of how close the lattice model we are considering comes to replicating LLL physics, and consequently, manifest an anomalous FQHE phase. Deviations in these conditions can be considered deviations from ideal behavior, and likelihood of manifesting an FCI phase.

Note that for an arbitrary n -dimensional matrix g , the AM-GM inequality applied to its eigenvalues gives us a simple relation, $\text{tr } g \geq n \cdot \sqrt{\det g}$. Combined with our determinant inequality, relating the quantum metric to the Berry curvature, we obtain $\text{tr } g \geq |\Omega_{12}|$ which places a weaker upper bound on the Chern number, $\int_{\text{BZ}} d^2k \cdot \text{tr } g \geq 2\pi|\mathcal{C}|$. Saturation of the trace inequality (known as the trace condition) implies that the Bloch states, $u_{\mathbf{k}}$ are holomorphic functions of $k_x + ik_y$, which provides us the simple form of the QGT [13]

$$Q \propto \begin{pmatrix} 1 & i \\ -i & 1 \end{pmatrix} \quad (73)$$

in which the quantum metric takes the simple form $g_{\mu\nu} \propto \delta_{\mu\nu}$, and the Berry curvature is also momentum-independent. It turns out that the trace condition combined with the uniformity of Berry curvature imply that the GMP algebra is reproduced.

In all, we have a few criteria regarding geometry that may hint at the manifestation of an FCI phase in our lattice model, termed the **Geometric Stability Hypothesis** [13, 9, 17, 19]

1. Berry curvature is constant,
2. Quantum metric is constant,
3. Determinant inequality is saturated (**determinant condition**, $\det g = |\Omega_{12}|^2/4$),
4. Trace inequality is saturated (**trace condition**, $\text{tr } g \geq |\Omega_{12}|$).

The trace condition (4) is stronger than the determinant condition (3), since it also requires the saturation of the AM-GM inequality for the eigenvalues of the quantum metric (although the inequality form is weaker). The determinant condition (3) holds if and only if $\det Q = 0$ and the Berry curvature does not change sign within the BZ (which is weaker than 1). Further, conditions (1) and (4) together imply (2), the quantum metric is constant, and therefore (1) and (4) imply both (2) and (3), and are the strongest of the conditions. We see that the more fundamental conditions are that Berry curvature is constant (1) and the trace conditions holds (4).

We define two quantities of interest for quantifying deviations from these ideal conditions (over the entire BZ)

$$\begin{aligned} T &\equiv \int_{\text{BZ}} d^2k \cdot |\text{tr } g - |\Omega_{12}||, \\ B &\equiv \left(\int_{\text{BZ}} d^2k \cdot (\Omega_{12}/2\pi - \mathcal{C})^2 \right)^{1/2}, \end{aligned} \quad (74)$$

where T captures deviations from the trace inequality and B captures deviations in the uniformity of Berry curvature.

The results for graphene, the Haldane model, and the checkerboard model are displayed in Figures 7, 8. The Haldane model has much more ideal bands with respect to the trace condition than the checkerboard model, however the former has a significantly lower (better) band-ratio (ratio of

band-width to band-gap). Thus it is not a priori clear which model is more likely to host FCI phases.

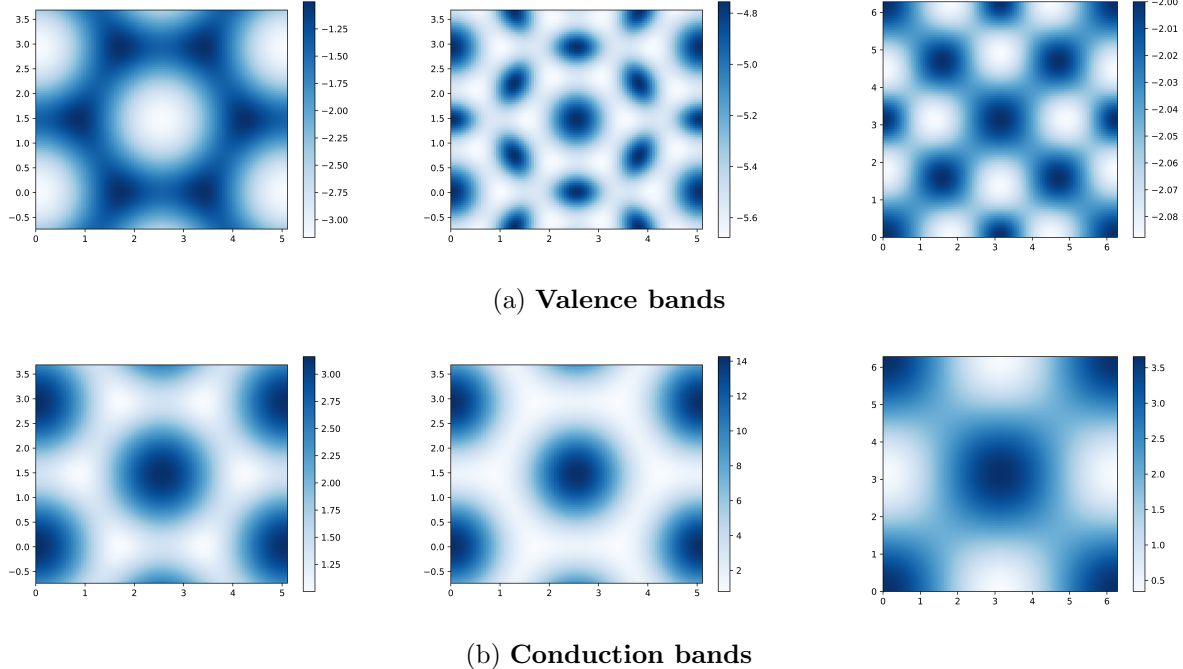


Figure 7: Valence and conduction bands of (left-to-right) graphene, the Haldane model, and the checkerboard model, respectively. We compute the ratio between the band-width (of the valence, flat band) to the band-gap as a measure of flatness of the band, and insignificance of Landau level mixing. For the Haldane mode, the band-width is $\Delta\varepsilon_0 = 0.7359$, the band-gap is $\Delta\varepsilon = 1.9561$, and the resulting ratio is $\Delta\varepsilon_0/\Delta\varepsilon = 0.3762$. For the checkerboard mode, the band-width is $\Delta\varepsilon_0 = 0.0877$, the band-gap is $\Delta\varepsilon = 2.3441$, and the resulting ratio is $\Delta\varepsilon_0/\Delta\varepsilon = 0.0374$. Therefore, we see that the band-ratio of the Haldane model is roughly $10\times$ that of the checkerboard model (lower is better).

5.2 Geometry-independence

The satisfaction of the conditions above have support from numerical simulations of FCI phases, but we cannot quite use conditions on the uniformity of the quantum metric or the Berry curvature as criteria to capture the manifestation of a phase.

To understand why Berry curvature (or its uniformity) cannot be an observable (a physical quantity), we must introduce the notion of geometry-independence. Consider a lattice with sublattice index α , and corresponding Wannier (orthonormal) basis $\{\alpha, \mathbf{R} + \mathbf{x}_\alpha\}$. The existence of this basis is the foundation of the tight-binding model. Without localized atomic orbitals, the tight-binding model does not capture the kinetic energy of electrons. The localization of atomic orbitals into point-like structures is a rather intuitive assumption, and will not qualitatively affect the results below. The requirement of point-like orbitals amounts to $\hat{\mathbf{r}}|\alpha, \mathbf{R} + \mathbf{x}_\alpha\rangle = (\mathbf{R} + \mathbf{x}_\alpha)|\alpha, \mathbf{R} + \mathbf{x}_\alpha\rangle$ where \mathbf{R} is the position of the unit cell, and \mathbf{x}_α is the position of the orbital relative to the unit cell. The orbital sites relative to the origin, $\mathbf{r}_{i\alpha} = \mathbf{R}_i + \mathbf{x}_\alpha$ are particular to the so-called orbital embedding we choose. As a slight tangent, it is important to understand the notion of embedding,

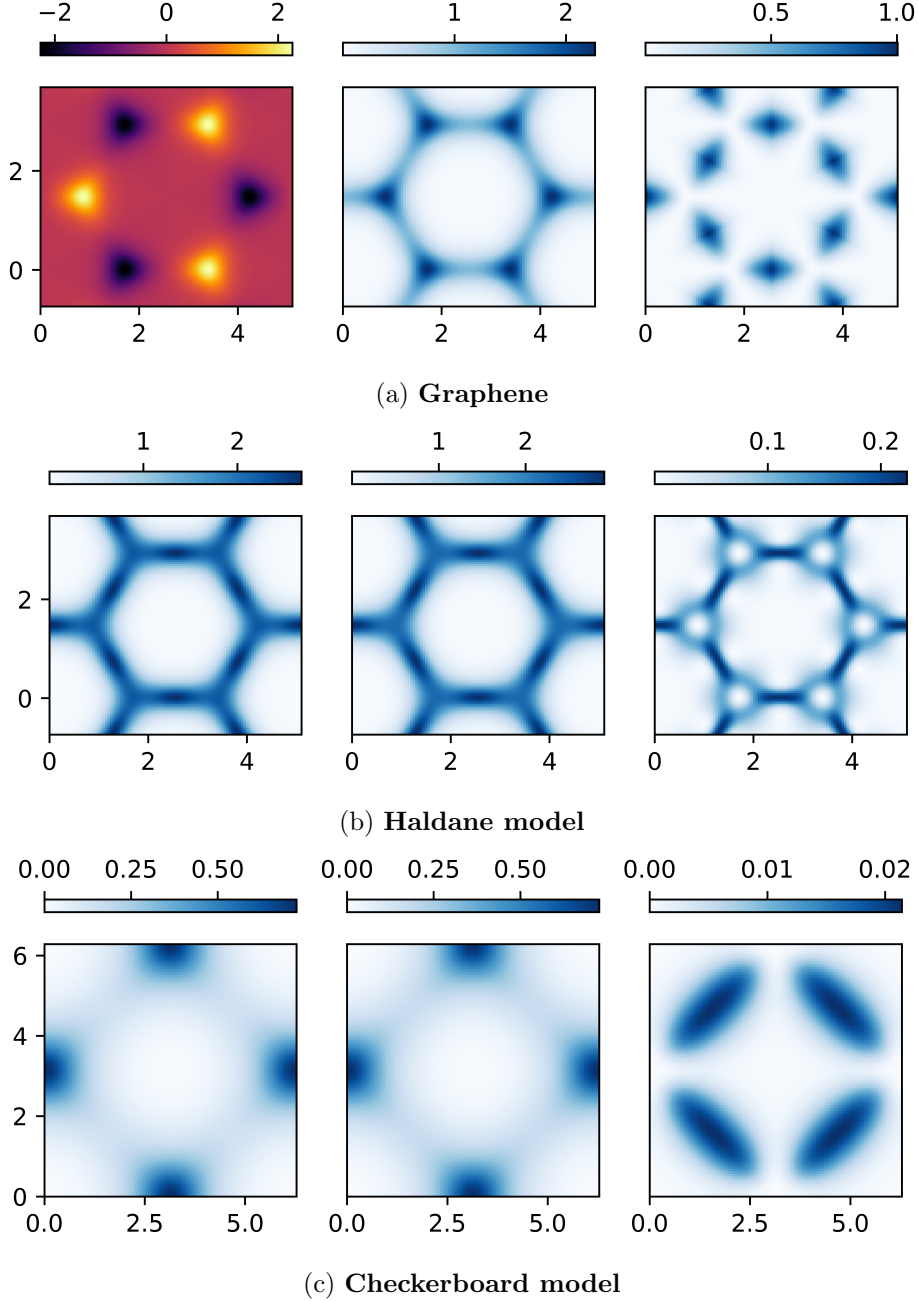


Figure 8: Berry curvature $\Omega_{12}(\mathbf{k})$, trace of quantum metric $\text{tr } g(\mathbf{k})$, and (local) deviation from trace condition $|\text{tr } g(\mathbf{k}) - |\Omega_{12}(\mathbf{k})||$ (left-to-right) for graphene, the Haldane model, and the checkerboard model. We compute the global deviations of uniformity of Berry curvature, and the trace condition, since these are the strongest proposed criteria on the geometry. For the checkerboard lattice, we compute the Chern number $\mathcal{C} = 1.0060$ (deviation from 1 due to not ideally designing the BZ), non-uniformity of Berry curvature $B = 6.1631$, and deviation from the trace condition $T = 0.5014$. For the Haldane model, we compute the Chern number $\mathcal{C} = 0.9883$ (deviation from 1 due to not ideally designing the BZ), non-uniformity of Berry curvature $B = 2.3812$, and deviation from the trace condition $T = 0.6395$.

or geometry in a broader context. Consider a manifold that is topologically a 2-sphere. Without specifically the geometry/metric of the manifold, or how it is embedded into a space, it is unknown how this manifold bends and twists, and may not correspond to our usual notion of a 2-sphere. Perhaps it is a sphere with a bump on the top. Similarly, the embedding of our lattice specifies the relative positions of orbitals the same way an embedding of a manifold specifies the relative position of its points with respect to the ambient space. Here we are strictly considering the term orbital as associated with a spatial location, instead of considering spin for instance. Using this Wannier basis, we can construct a tight-binding model for the lattice

$$H = \sum_{ij} t_{ij} c_i^\dagger c_j + h.c. \quad (75)$$

where $h.c. = c_j^\dagger c_i$. Note that at the end of the process, all information about the orbital positions has been abstracted away in favor of the hopping parameters t_{ij} . In a clear sense, the information of the Hamiltonian is completely encoded in an undirected, weighted graph where the vertices correspond to the lattice sites, and the edges correspond to the associated hopping amplitude, t_{ij} . Note that for the Haldane model which breaks time-reversal symmetry to achieve non-zero Chern number, the graph becomes directed. It is also intuitive, as in the case of the Haldane model, that a directed graph manifestly breaks time-reversal symmetry as all the directions revert under the reversal of time.

The natural quantities that can be derived from the Hamiltonian, such as band-structure and eigenstates only explicitly depend on the graph weights t_{ij} and not on the orbital positions. Note that in a physical sense, the weights t_{ij} do implicitly depend on the orbital positions. For instance, if we were to physically stretch the lattice in one direction, the hopping amplitudes in that direction would increase, as it is presumably more difficult for electrons to hop in a stretched direction, since the orbital positions are further apart. However, this dependence is only implicit, and of course, we can choose any magnitude of hopping amplitudes as long as they obey the symmetries of the system. For a square lattice for instance, we cannot assign a higher hopping amplitude for the vertical direction relative to the horizontal direction. Nevertheless, as theorists, we have some freedom in choosing these hopping amplitudes, or graph weights. If we also considered an interaction with weights U_{ij} or on onsite term with weights t_{ii} , then **geometry-independent** quantities are precisely those that can only depend on these quantities, and not explicitly on orbital positions [19]. Moreover, it is clear that the many-body gap induced by an interaction is also geometry-independent, as it is solely dependent on the weights. On the other hand, quantities that do explicitly depend on the orbital positions are called **geometry-dependent**. Consider the eigenstates of the Hamiltonian

$$|\psi_n(\mathbf{k})\rangle = \sum_{\alpha} \psi_{n\alpha}(\mathbf{k}) |\alpha, \mathbf{k}\rangle, \quad |\alpha, \mathbf{k}\rangle = \sum_{\mathbf{R}} e^{i\mathbf{k}\cdot\mathbf{R}} |\alpha, \mathbf{R} + \mathbf{x}_{\alpha}\rangle \quad (76)$$

where $\psi_{n\alpha}$ are the scalar amplitudes of the eigenstate. Consequently, we expect these quantities, $\psi_{n\alpha}$ to be geometry-independent since we can compute them using the Hamiltonian, which is geometry-independent. It would be a bit incorrect to claim that the eigenstates themselves are geometry-independent since they depend on a choice of Wannier basis. However, with this basis fixed, the amplitudes of the eigenstates are indeed geometry-independent. Similarly, the spectrum is also geometry-independent. The shifting of orbital positions corresponds to a unitary transformation on the Hamiltonian (change of basis), and since it is unitary, the spectrum is left invariant.

One may naively conclude that every quantity is geometry-independent since the Hamiltonian is so, but we would be wrong, and neglecting one of the fundamental theorems of condensed matter physics, the Bloch theorem. Recalling from earlier, this theorem assumes an external (ionic) periodic potential in two-dimensions and concludes that the eigenstates, $|\psi_{n,\mathbf{k}}(\mathbf{r})\rangle$ of the Hamiltonian have the form

$$|\psi_{n,\mathbf{k}}(\mathbf{r})\rangle = e^{i\mathbf{k}\cdot\mathbf{r}} |u_{n,\mathbf{k}}(\mathbf{r})\rangle, \quad |u_{n,\mathbf{k}}(\mathbf{r} + \mathbf{a}_j)\rangle = |u_{n,\mathbf{k}}(\mathbf{r})\rangle \quad (77)$$

where $u_{n,\mathbf{k}}(\mathbf{r})$ is called the Bloch function, and \mathbf{a}_j are the primitive vectors of the lattice. We see that the form of $f_{n,\mathbf{k}}(\mathbf{r})$ is that of a plane-wave modulated by a function periodic in the unit cell. Note that by requiring the eigenstates to have the same periodicity of the lattice, the eigenstates become explicitly dependent on the orbital positions. The above expressions can be written in momentum-space $|\psi_n(\mathbf{k})\rangle = e^{i\mathbf{k}\cdot\hat{\mathbf{r}}} |u_n(\mathbf{k})\rangle$ where $\hat{\mathbf{r}}$ is the position operator. We can expand the Bloch function as a Fourier series to evaluate the action of the position operator [19]

$$\hat{\mathbf{r}} |u_n(\mathbf{k})\rangle = \sum_{\mathbf{R},\alpha} u_{n\alpha}(\mathbf{k}) \hat{\mathbf{r}} |\alpha, \mathbf{R} + \mathbf{x}_\alpha\rangle = \sum_{\mathbf{R},\alpha} u_{n\alpha}(\mathbf{k}) (\mathbf{R} + \mathbf{x}_\alpha) |\alpha, \mathbf{R} + \mathbf{x}_\alpha\rangle = (\mathbf{R} + \mathbf{x}_\alpha) |u_n(\mathbf{k})\rangle \quad (78)$$

and therefore we have $|\psi_n(\mathbf{k})\rangle = e^{i\mathbf{k}\cdot(\mathbf{R} + \mathbf{x}_\alpha)} |u_n(\mathbf{k})\rangle = e^{i\mathbf{k}\cdot\mathbf{x}_\alpha} |u_n(\mathbf{k})\rangle$ where we used that $e^{i\mathbf{k}\cdot\mathbf{R}}$ in the second equality. Hence, we see that the Bloch function amplitudes $u_{n\alpha}(\mathbf{k})$ are geometry-dependent. Recall that the quantities that capture quantum geometry, such as the Berry connection and curvature, are defined in terms of Bloch functions, and are therefore generally geometry-dependent.

Consider two systems X, Y that have the same tight-binding parameters t_{ij} but with different orbital embeddings, $\{\mathbf{x}_\alpha\}$. We define the relative displacement vector $\delta\mathbf{x}_\alpha = \mathbf{x}_\alpha^X - \mathbf{x}_\alpha^Y$, and relate their Bloch functions [19]

$$u_{n\alpha}^Y(\mathbf{k}) = e^{-i\mathbf{k}\cdot\delta\mathbf{x}_\alpha} u_{n\alpha}^X(\mathbf{k}) \quad (79)$$

which is derived immediately from our prior considerations. Note that this quantity appears similar in form to a gauge transformation, with one crucial distinction, it distinguishes between sublattice. A gauge transformation (in momentum space) can be expressed as $e^{-i\Lambda(\mathbf{k})}$ for some well-behaved function $\Lambda(\mathbf{k})$. Gauge transformations such as with gauge function $\Lambda(\mathbf{k})$ cannot depend on sublattice, and this detail is necessary for the considerations below. Continuing, with this orbital displacement Berry connection transforms as [19]

$$\mathcal{A}_\mu^Y(\mathbf{k}) = \mathcal{A}_\mu^X(\mathbf{k}) + \overline{\delta\mathbf{x}_n}(\mathbf{k}) \quad (80)$$

where

$$\overline{\delta\mathbf{x}_n}(\mathbf{k}) = \sum_\alpha \delta\mathbf{x}_\alpha |u_{n\alpha}(\mathbf{k})|^2 \quad (81)$$

can be interpreted as a momentum-dependent shift in the electron position within the unit cell [19]. The Berry curvature then transforms as [19]

$$\Omega_\mu^Y(\mathbf{k}) = \Omega_\mu^X(\mathbf{k}) + (\nabla_\mathbf{k} \times \overline{\delta\mathbf{x}_n}(\mathbf{k}))_\mu. \quad (82)$$

There are a few important points to take note of. Most obviously, the Berry curvature transforms as the curl of a function, and therefore, the Chern number is left invariant since the integral of a curl over a manifold (BZ) with no boundary vanishes, $\Delta\mathcal{C} = \int_{\text{BZ}} d^2\mathbf{k} \cdot \nabla_\mathbf{k} \times \overline{\delta\mathbf{x}_n}(\mathbf{k}) = 0$. Since the Berry curvature is explicitly dependent on orbital position, it is geometry-independent and thus is not a physical observable, although its integral, the Chern number is related to the Hall conductivity and is a physical observable. Since the Berry curvature is geometry-dependent, its characteristics should

not be used as criterion for the manifestation of a phase. In addition, other related quantities, such as the uniformity (standard deviation) of the Berry curvature are also geometry-dependent and can be changed via shifting of orbital position, while the Hamiltonian is left unchanged.

The shifting of orbital position cannot quite be referred to as a type of gauge transformation since the physical system is genuinely changing, but the quantities of interest to us do not necessarily change since they are not explicitly dependent on the orbital embedding [19]. Therefore, while the structure of the transformation is similar, the sublattice-dependence on the analogous gauge function ruins the analogy, and the transformation is not a true gauge transformation as the physical system has changed.

To recap, criteria for manifestation of FCI phases (or any phase) cannot be dependent on geometry-dependent quantities such as the (uniformity of) Berry curvature, or the trace condition. Nonetheless, numerical simulations support that these conditions are relevant criteria. One proposed solution is to optimize these quantities over all possible geometries (orbital positions), and then deviations of these quantities from ideal conditions should be used as criteria. For instance, we define the manifestly geometry-independent trace condition

$$\tilde{T} \equiv \min_{\mathbf{x}^Y} \left(\int_{\text{BZ}} d^2k \cdot |\text{tr } g - |\Omega_{12}|| \right) \quad (83)$$

and the uniformity of Berry curvature

$$\tilde{B} \equiv \min_{\mathbf{x}^Y} \left(\int_{\text{BZ}} d^2k \cdot (\Omega_{12}^Y/2\pi - \mathcal{C})^2 \right)^{1/2}, \quad (84)$$

as relevant criteria [19, 13]. Although these quantities are geometry-independent, it is not obvious how to motivate them on physical grounds. The lattice has a particular geometry, and although the criteria for manifesting a particular phase cannot depend on this geometry, it seems unphysical to optimize over all geometries, as you are losing information pertaining to the lattice. Therefore, although we have poked a hole in the geometry-dependence of the Geometric Stability Hypothesis, we do not have a clear, useful alternative. In recent literature, the idea of vortexability of bands has been of interest, but we will not review these concepts as they do not pertain to our numerical simulations [13].

6 Numerical Techniques for Simulating Fractional Chern Insulators

The motivation and theory of fractional Chern insulators (FCI) has been thoroughly developed. We now shift our attention to numerically simulating these phases by adding simple repulsive interactions to Chern insulators. Recall that the manifestation of Chern insulators only requires non-trivial topology, and there are not stringent criteria on the geometry of the model.³⁷ The FCI requires careful tuning of parameters to first achieve an approximate flat band. Flat bands enable interactions to dominate over the kinetic energy. There are then requirements of quantum geometry, but as we saw in the previous section, they may not be necessary (or even relevant on physical grounds).

³⁷Of course, the geometry and topology are connected. There are no geometric criteria for Chern insulators which are unrelated to achieving a non-zero Chern number.

The aim is to set up the combined Hamiltonian (the Chern insulator model combined with the repulsive interaction), and diagonalize it. This generic procedure is called **exact-diagonalization (ED)** and is used throughout computational condensed matter physics to solve for the spectrum of highly-interacting models. ED is also used for solving non-interacting models, but its use there is more trivial. The resulting Hamiltonian will be very large, but also sparse, so we can utilize Lanczos's numerical, iterative diagonalization protocol to solve for the smallest (algebraic) eigenvalues and eigenstates. We will compute these eigenvalues, and search for degeneracy in the ground state manifold, an indication of the FQHE, which we take to be an indication of the FCI. The degeneracy was the result of topological considerations and is therefore a robust measure of the manifestation of the FCI phase.

6.1 Single-band approximation of many-body Hamiltonian

We consider the nearest-neighbor (NN) interaction on the (real-space) lattice [16, 18]

$$H_{\text{NN}} = U \sum_{\langle i\alpha, j\beta \rangle} n_{i\alpha} n_{j\beta} \quad (85)$$

where $n_{i\alpha} = c_{i\alpha}^\dagger c_{i\alpha}$ is the number operator, representing the presence of a fermion on lattice site i and sublattice α . The requirement of fixed particle number, N_p amounts to applying the constraint $\sum_{i\alpha} n_{i\alpha} = N_p$ where $\langle n_{i\alpha} \rangle \in [0, 1]$. We could also leave the particle number as a parameter tuned by the chemical potential, μ , by including the term $\mu \sum_{i\alpha} n_{i\alpha}$ in the Hamiltonian.

We intend to diagonalize this interaction. Since the lattice is periodic, it is convenient to change bases into momentum space

$$c_{i\alpha}^\dagger = \frac{1}{\sqrt{N_s}} \sum_{\mathbf{k}} e^{-i\mathbf{k}\cdot\mathbf{R}_\alpha^i} c_{\mathbf{k}\alpha}^\dagger \quad (86)$$

where α is the sublattice index and $N_s = N_x \cdot N_y$ is the number of unit cells. We apply this expansion to each fermionic operator in the interaction to obtain

$$H_{\text{NN}} = \frac{U}{N_s^2} \sum_{\langle i\alpha, j\beta \rangle} \sum_{\mathbf{k}_1, \mathbf{k}_2, \mathbf{k}_3, \mathbf{k}_4} e^{-i\mathbf{k}_1 \cdot \mathbf{R}_\alpha^i} e^{-i\mathbf{k}_2 \cdot \mathbf{R}_\beta^j} e^{i\mathbf{k}_3 \cdot \mathbf{R}_\alpha^j} e^{i\mathbf{k}_4 \cdot \mathbf{R}_\beta^j} \cdot c_{\mathbf{k}_1\alpha}^\dagger c_{\mathbf{k}_2\beta}^\dagger c_{\mathbf{k}_3\alpha} c_{\mathbf{k}_4\beta} \quad (87)$$

where we assume i corresponds to sublattice α , and j to β . The requirement that i, j be nearest neighbors amounts to $\mathbf{R}_\beta^j = \mathbf{R}_\alpha^i + \boldsymbol{\tau}_{\alpha\beta}$ where $\boldsymbol{\tau}_{\alpha\beta}$ denotes a nearest-neighbor hopping vector from sublattice α to β . For the checkerboard lattice, there are four such vectors, and they are independent of which direction the electron is hopping, $\boldsymbol{\tau}_{\alpha\beta} = \boldsymbol{\tau}$. However, we keep the notation since this is not generally true (e.g. honeycomb lattice).

Substituting this relation, we obtain

$$\begin{aligned} H_{\text{NN}} &= \frac{U}{N_s^2} \sum_{\mathbf{k}_1, \mathbf{k}_2, \mathbf{k}_3, \mathbf{k}_4} \sum_{\alpha, \beta; \alpha \neq \beta} \sum_{\boldsymbol{\tau}_{\alpha\beta}} \sum_{\mathbf{R}_\alpha} e^{i\mathbf{R}_\alpha^i \cdot (\mathbf{k}_3 + \mathbf{k}_4 - \mathbf{k}_1 - \mathbf{k}_2)} \cdot e^{-i\boldsymbol{\tau}_{\alpha\beta} \cdot (\mathbf{k}_2 - \mathbf{k}_4)} \cdot c_{\mathbf{k}_1\alpha}^\dagger c_{\mathbf{k}_2\beta}^\dagger c_{\mathbf{k}_3\alpha} c_{\mathbf{k}_4\beta} \\ &= \frac{U}{N_s} \sum_{\mathbf{k}_1, \mathbf{k}_2, \mathbf{k}_3, \mathbf{k}_4} \sum_{\alpha, \beta; \alpha \neq \beta} \sum_{\boldsymbol{\tau}_{\alpha\beta}} \delta_{\mathbf{k}_3 + \mathbf{k}_4 - \mathbf{k}_1 - \mathbf{k}_2} \cdot e^{-i\boldsymbol{\tau}_{\alpha\beta} \cdot (\mathbf{k}_2 - \mathbf{k}_4)} \cdot c_{\mathbf{k}_1\alpha}^\dagger c_{\mathbf{k}_2\beta}^\dagger c_{\mathbf{k}_3\alpha} c_{\mathbf{k}_4\beta} \\ &= \frac{U}{N_s} \sum_{\mathbf{k}_1, \mathbf{k}_2, \mathbf{k}_4} \sum_{\alpha, \beta; \alpha \neq \beta} \left(\sum_{\boldsymbol{\tau}_{\alpha\beta}} e^{-i\boldsymbol{\tau}_{\alpha\beta} \cdot (\mathbf{k}_2 - \mathbf{k}_4)} \right) \cdot c_{\mathbf{k}_1\alpha}^\dagger c_{\mathbf{k}_2\beta}^\dagger c_{(\mathbf{k}_1 + \mathbf{k}_2 - \mathbf{k}_4)\alpha} c_{\mathbf{k}_4\beta} \end{aligned} \quad (88)$$

where in the second line we used the identity, $\sum_{\mathbf{R}} e^{i\mathbf{R} \cdot \mathbf{k}} = N \cdot \delta_{\mathbf{k}}$ which is derived by using the particular form of \mathbf{k} . We use the short-hand Kronecker-delta notation $\delta_{\mathbf{k}} = \delta_{k_x,0}\delta_{k_y,0}$.

A natural basis corresponds to $|\mathbf{k}_1\alpha_1, \dots, \mathbf{k}_{N_p}\alpha_{N_p}\rangle$, where each particle has a momentum and sub-lattice. Under periodic boundary conditions, the single-particle momentum is quantized along each direction, $k_x = 2\pi n/(a_0 N_x)$, $k_y = 2\pi m/(a_0 N_y)$ where $n \in \{0, 1, \dots, N_x - 1\}$, $m \in \{0, 1, \dots, N_y - 1\}$. We denote the number of unit cells as $N_s = N_x \cdot N_y$. Due to (lattice) translational invariance (we are using periodic boundary conditions), the Hamiltonian does not couple states with different total momentum, $\mathbf{K} \equiv \sum_i \mathbf{k}_i$ where \mathbf{k}_i , $i \in \{1, \dots, N\}$ are the single-particle momenta of the N -particle state. This allows us to reduce the size of the problem since the Hamiltonian is block-diagonal with respect to \mathbf{K} .

One additional point to take note of is that the particles (fermions) are indistinguishable, and so we can exchange indices as long as we include the appropriate sign. Consequently, our basis is not a permutation of the N_s single-particle momentum states but is a combination of them (order does not matter).

The total number of single-particle momentum states is N_s and so the total number of N_p -particle momentum states is $\binom{N_s}{N_p}$, which when we restrict to a single momentum-sector roughly becomes $d_k \equiv \binom{N_s}{N_p}/N_s$. In the above case of the 4×6 checkerboard lattice model with 8 electrons, we have $d_k \approx 31,000$.

With the inclusion of the orbital degree of freedom, this dimension is scaled by $d_\alpha \equiv N_{\text{orb}}^{N_p}$ where N_{orb} is the number of orbitals, or sublattices. In the above case, we have $d_\alpha = 2^8 = 256$, and therefore the total size of the system becomes roughly $d \equiv d_k \cdot d_\alpha = \binom{N_s}{N_p} \cdot N_{\text{orb}}^{N_p}/N_s \approx 7,860,000$, corresponding to a matrix of size $d \times d$ with roughly 10^{14} complex elements. Although this matrix is presumably sparse, it still contains an excessive amount of information, and both its initialization and diagonalization would be significantly challenging for the typical computer. Therefore, we aim to reduce the size of the system by projecting the interaction only to the lowest one-body band, effectively setting $N_{\text{orb}} = 1$ and so $d = d_k$. This approximation is only appropriate given that the interaction strength is much smaller than the band-gap $U \ll \min_{\mathbf{k}}(\varepsilon_1(\mathbf{k}) - \varepsilon_0(\mathbf{k}))$ and the interaction strength is much larger than the band-width $U \gg \max_{\mathbf{k}, \mathbf{k}'}(\varepsilon_0(\mathbf{k}) - \varepsilon_0(\mathbf{k}'))$. The first condition naturally ensures the interaction-induced scattering of states between one-body energy bands is negligible, and therefore we are justified in ignoring higher one-body energy bands. The second condition ensures that within the lowest band, the interaction is dominant over the kinetic energy.

Let $u_{n\mathbf{k}}$ be the single-particle (non-interacting) eigenstates, $H_0(\mathbf{k})u_{n\mathbf{k}} = \varepsilon_{n\mathbf{k}}u_{n\mathbf{k}}$ where we denote the vector indices with superscript. We now project the fermion operators onto the lowest band. The projection operator can be naturally expressed as $P_{\mathbf{k}} = |u_{0\mathbf{k}}\rangle\langle u_{0\mathbf{k}}| = u_{0\mathbf{k}}u_{0\mathbf{k}}^\dagger$. As expected from a projection operator, it is idempotent ($P_{\mathbf{k}}^2 = P_{\mathbf{k}}$) and Hermitian ($P_{\mathbf{k}}^\dagger = P_{\mathbf{k}}$). The projected fermion creation operators can be expressed [1]

$$\tilde{\mathbf{c}}_{\mathbf{k}}^\dagger = \mathbf{c}_{\mathbf{k}}^\dagger P_{\mathbf{k}} = (\mathbf{c}_{\mathbf{k}}^\dagger u_{0\mathbf{k}}) \cdot u_{0\mathbf{k}}^\dagger = (\bar{u}_{0\mathbf{k}}^1 f_{\mathbf{k}}^\dagger, \bar{u}_{0\mathbf{k}}^2 f_{\mathbf{k}}^\dagger) \quad (89)$$

where $f_{\mathbf{k}}^\dagger = \mathbf{c}_{\mathbf{k}}^\dagger u_{0\mathbf{k}}$ is the creation operator of the lowest band eigenstate. Bold fermion operators denotes the vector of fermion operators, $\mathbf{c}_{\mathbf{k}}^\dagger = (c_{\mathbf{k}A}^\dagger, c_{\mathbf{k}B}^\dagger)$ and $\tilde{\mathbf{c}}_{\mathbf{k}}^\dagger = (\tilde{c}_{\mathbf{k}A}^\dagger, \tilde{c}_{\mathbf{k}B}^\dagger)$, and correspondingly for the annihilation operators. The projected annihilation operators can be derived from taking the Hermitian-conjugate of the above, $\tilde{\mathbf{c}}_{\mathbf{k}} = (u_{0\mathbf{k}}^1 f_{\mathbf{k}}, u_{0\mathbf{k}}^2 f_{\mathbf{k}})$.

We compute the anti-commutation relations to prove that the projected operators are also fermionic,

$$\begin{aligned}
\{f_{\mathbf{k}_i}^\dagger, f_{\mathbf{k}_j}\} &= \{c_{\mathbf{k}_i}^\dagger \cdot u_{0\mathbf{k}_i}, c_{\mathbf{k}_j} \cdot \bar{u}_{0\mathbf{k}_j}\} \\
&= \{u_{0\mathbf{k}_i}^A c_{\mathbf{k}_i A}^\dagger + u_{0\mathbf{k}_i}^B c_{\mathbf{k}_i B}^\dagger, \bar{u}_{0\mathbf{k}_j}^A c_{\mathbf{k}_j A} + \bar{u}_{0\mathbf{k}_j}^B c_{\mathbf{k}_j B}\} \\
&= u_{0\mathbf{k}_i}^A \bar{u}_{0\mathbf{k}_j}^A \{c_{\mathbf{k}_i A}^\dagger, c_{\mathbf{k}_j A}\} + u_{0\mathbf{k}_i}^B \bar{u}_{0\mathbf{k}_j}^B \{c_{\mathbf{k}_i B}^\dagger, c_{\mathbf{k}_j B}\} \\
&= \delta_{ij} (u_{0\mathbf{k}_i}^A \bar{u}_{0\mathbf{k}_j}^A + u_{0\mathbf{k}_i}^B \bar{u}_{0\mathbf{k}_j}^B) = \delta_{ij}
\end{aligned} \tag{90}$$

where in the last equality we used that in the case of $i = j$, the coefficient becomes unity since $u_{0\mathbf{k}}^\dagger u_{0\mathbf{k}} = 1$. It is clear that $\{f_{\mathbf{k}_i}, f_{\mathbf{k}_j}\} = \{f_{\mathbf{k}_i}^\dagger, f_{\mathbf{k}_j}^\dagger\} = 0$.

In the case of the momentum-space two-body interaction we are considering, the projection can be obtained

$$c_{\mathbf{k}_1\alpha}^\dagger c_{\mathbf{k}_2\beta}^\dagger c_{\mathbf{k}_3\alpha} c_{\mathbf{k}_4\beta} \mapsto \tilde{c}_{\mathbf{k}_1\alpha}^\dagger \tilde{c}_{\mathbf{k}_2\beta}^\dagger \tilde{c}_{\mathbf{k}_3\alpha} \tilde{c}_{\mathbf{k}_4\beta} = \overline{u_{0\mathbf{k}_1}^\alpha u_{0\mathbf{k}_2}^\beta} u_{0\mathbf{k}_3}^\alpha u_{0\mathbf{k}_4}^\beta \cdot f_{\mathbf{k}_1}^\dagger f_{\mathbf{k}_2}^\dagger f_{\mathbf{k}_3} f_{\mathbf{k}_4} \tag{91}$$

where sublattice $A(B)$ corresponds to vector index 1(2). From a purely computational perspective, we are transferring the sublattice index from the basis into a scalar sum, and thus the basis size reduces substantially (by $N_{\text{orb}}^{N_p}$). Note that projection and (anti-)commutation of fermion operators are generally not commuting operations. Consider the two-body scattering term $c_{\mathbf{k}_1\alpha}^\dagger c_{\mathbf{k}_2\beta}^\dagger c_{\mathbf{k}_3\alpha} c_{\mathbf{k}_4\beta}$. If we anti-commuted this term to obtain, $c_{\mathbf{k}_1\alpha}^\dagger c_{\mathbf{k}_3\alpha} c_{\mathbf{k}_2\beta}^\dagger c_{\mathbf{k}_4\beta}$ (since $\alpha \neq \beta$), and then projected onto the flat band, we would obtain

$$\overline{u_{0\mathbf{k}_1}^\alpha u_{0\mathbf{k}_2}^\beta} u_{0\mathbf{k}_3}^\alpha u_{0\mathbf{k}_4}^\beta \cdot f_{\mathbf{k}_1}^\dagger f_{\mathbf{k}_3} f_{\mathbf{k}_2}^\dagger f_{\mathbf{k}_4}, \tag{92}$$

which amounts to the same scalar factor, but with a different permutation of projected fermion operators. We we anti-commute to obtain the same order as the case above, we would obtain an extra term

$$\overline{u_{0\mathbf{k}_1}^\alpha u_{0\mathbf{k}_2}^\beta} u_{0\mathbf{k}_3}^\alpha u_{0\mathbf{k}_4}^\beta \cdot f_{\mathbf{k}_1}^\dagger f_{\mathbf{k}_2}^\dagger f_{\mathbf{k}_3} f_{\mathbf{k}_4} - |u_{0\mathbf{k}_1}^\alpha u_{0\mathbf{k}_1}^\beta|^2 \cdot f_{\mathbf{k}_1}^\dagger f_{\mathbf{k}_1} \tag{93}$$

where we used $\{f_{\mathbf{k}_3}^\dagger, f_{\mathbf{k}_2}\} = \delta_{\mathbf{k}_3, \mathbf{k}_2}$, and that $\mathbf{k}_3 = \mathbf{k}_2$ implies that $\mathbf{k}_1 = \mathbf{k}_4$. The first term matches the term we obtained before from projection, but the second term is entirely new. The fermion operators must be normal-ordered prior to projection.

Substituting the eigenbasis approximation into the interaction term, we obtain

$$H_{\text{NN}} = - \sum_{\mathbf{k}_1, \mathbf{k}_2, \mathbf{k}_4} \left(U_{\mathbf{k}_1 \mathbf{k}_2 (\mathbf{k}_1 + \mathbf{k}_2 - \mathbf{k}_4) \mathbf{k}_4} \cdot f_{\mathbf{k}_1}^\dagger f_{\mathbf{k}_2}^\dagger f_{(\mathbf{k}_1 + \mathbf{k}_2 - \mathbf{k}_4)} f_{\mathbf{k}_4} \right) \tag{94}$$

where

$$U_{\mathbf{k}_1 \mathbf{k}_2 \mathbf{k}_3 \mathbf{k}_4} = \frac{U}{N_s} \sum_{\alpha, \beta; \alpha \neq \beta} \left(\overline{u_{0\mathbf{k}_1}^\alpha u_{0\mathbf{k}_2}^\beta} u_{0\mathbf{k}_3}^\alpha u_{0\mathbf{k}_4}^\beta \cdot \sum_{\boldsymbol{\tau}_{\alpha\beta}} e^{-i\boldsymbol{\tau}_{\alpha\beta} \cdot (\mathbf{k}_2 - \mathbf{k}_4)} \right). \tag{95}$$

In the case of the checkerboard lattice, the hoppings vectors are invariant of sublattice direction, and so the sum factors

$$U_{\mathbf{k}_1 \mathbf{k}_2 \mathbf{k}_3 \mathbf{k}_4} = \frac{U}{N_s} \sum_{\alpha, \beta; \alpha \neq \beta} \overline{u_{0\mathbf{k}_1}^\alpha u_{0\mathbf{k}_2}^\beta} u_{0\mathbf{k}_3}^\alpha u_{0\mathbf{k}_4}^\beta \cdot \sum_{\boldsymbol{\tau}} e^{-i\boldsymbol{\tau} \cdot (\mathbf{k}_2 - \mathbf{k}_4)} \tag{96}$$

It is also important to take note that all momenta are defined with respect to the modulo relation

provided earlier (in particular when combining momenta). The above formula is general and applies to any lattice model provided you input the proper hopping vectors and eigenstates.

For the checkerboard lattice, we have the evaluation $\sum_{\tau} e^{-i\tau \cdot (\mathbf{k}_2 - \mathbf{k}_4)} = 4 \cos((k_2^x - k_4^x)/2) \cdot \cos((k_2^y - k_4^y)/2)$ where v^i denotes the i^{th} component of the vector, not to be confused with particle indices, x, y .

Expressing the non-interacting tight-binding Hamiltonian in this basis, we would expect

$$H_0 = \sum_{\mathbf{k}} \sum_{\alpha\beta} H(\mathbf{k})_{\alpha\beta} c_{\mathbf{k}\alpha}^\dagger c_{\mathbf{k}\beta} \mapsto \sum_{\mathbf{k}} \varepsilon_{0\mathbf{k}} f_{\mathbf{k}}^\dagger f_{\mathbf{k}} \quad (97)$$

where we can also obtain the final approximation by substituting the approximate eigenbasis transformation for the fermion operators described above. To see this explicitly, note that since $H(\mathbf{k})u_{0\mathbf{k}} = \varepsilon_{0\mathbf{k}} u_{0\mathbf{k}}$, using the normality of the eigenbasis, we have $\langle u_{0\mathbf{k}} | H(\mathbf{k}) | u_{0\mathbf{k}} \rangle = u_{0\mathbf{k}}^\dagger H(\mathbf{k}) u_{0\mathbf{k}} = \varepsilon_{0\mathbf{k}}$ where the middle term is also derived from the substitution of the basis transformation

$$H_0 \mapsto \sum_{\mathbf{k}} \left(\sum_{\alpha\beta} H(\mathbf{k})_{\alpha\beta} \cdot \overline{u_{0\mathbf{k}}^\alpha} u_{0\mathbf{k}}^\beta \right) f_{\mathbf{k}}^\dagger f_{\mathbf{k}}. \quad (98)$$

This **single-band approximation** projects the dynamics onto the lowest band. The procedure produces a similar outcome to that of Renormalization. However, instead of projecting out irrelevant modes, they are averaged over in the Renormalization procedure.

Using the formalism above we can also consider next-nearest-neighbor (NNN) interactions

$$H_{\text{NNN}} = -V \sum_{\langle\langle i\alpha, j\alpha \rangle\rangle} n_{i\alpha} n_{j\alpha} \quad (99)$$

where the NNN requirement simply manifests as requiring $\alpha = \beta$ when compared to the NN interaction. Projecting this NNN interaction onto the lowest band, we obtain the projected interaction

$$V_{\mathbf{k}_1 \mathbf{k}_2 \mathbf{k}_3 \mathbf{k}_4} = \frac{V}{N_s} \sum_{\alpha} \left(\overline{u_{0\mathbf{k}_1}^\alpha} \overline{u_{0\mathbf{k}_2}^\alpha} u_{0\mathbf{k}_3}^\alpha u_{0\mathbf{k}_4}^\alpha \cdot \sum_{\tau_{\alpha\alpha}} e^{-i\tau_{\alpha\alpha} \cdot (\mathbf{k}_2 - \mathbf{k}_4)} \right). \quad (100)$$

We can also consider higher-body terms such as the nearest-neighbor three-body interaction

$$H_{\text{NN}}^2 = U_2 \sum_{\langle\langle i\alpha, j\beta, k\gamma \rangle\rangle} n_{i\alpha} n_{j\beta} n_{k\gamma}. \quad (101)$$

Note that all three particles must be nearest-neighbors. We will not consider such interactions as the two-body interaction suffices, but it is important to keep in mind that higher-body interactions do play a role in the physics.

Due to the projection onto the flat band, the results are not completely accurate, depending on our choice of interaction-scale U .

6.2 Issues with uniformly choosing gauge

We now discuss computational difficulties that may arise when trying to compute the above Hamiltonian, and methods of resolving them. To preface, we recall the equation we derived earlier for the Berry curvature, $\Omega_{\mu\nu}^{(n)}(\mathbf{k}) = -2\text{Im} \langle \partial_\mu u_{n\mathbf{k}} | \partial_\nu u_{n\mathbf{k}} \rangle$, which involves the eigenvectors, $u_{n\mathbf{k}}$. When

we solve for these eigenvectors, there is a degree of freedom resulting in an arbitrary phase. Note that if $|v\rangle$ is an eigenvector of A ($A|v\rangle = \lambda|v\rangle$), then we also have that $e^{i\phi}|v\rangle$ is also an eigenvector (it is in the same one-dimensional eigenspace), $A(e^{i\phi}|v\rangle) = \lambda(e^{i\phi}|v\rangle)$. Each time you solve for an eigenvector, its phase is not certain. This becomes problematic when a single expression requires computations of distinct eigenvectors. For instance, when numerically computing the derivative required in the expression for the Berry curvature, we may obtain [2]

$$\partial_m u_{n\mathbf{k}} = \lim_{\Delta k \rightarrow 0} \frac{1}{\Delta k} (e^{i\phi_1} u_{n(\mathbf{k} + \hat{\mu}\Delta k)} - e^{i\phi_2} u_{n\mathbf{k}}) \quad (102)$$

where ϕ_1 and ϕ_2 are arbitrary, ruining the computation. We need to find a smooth gauge. At the present stage, the eigenstates are not smooth with respect to the continuous variable \mathbf{k} .

In the case of Berry curvature, this issue can be resolved by shifting the derivatives from the Bloch functions to the Hamiltonian [2]. To see how this is accomplished, consider the eigenstate equation $H|n\rangle = \varepsilon_n|n\rangle$, and differentiate both sides to obtain $(\partial_\mu H)|n\rangle + H|\partial_\mu n\rangle = (\partial_\mu \varepsilon_n)|n\rangle + \varepsilon_n|\partial_\mu n\rangle$. We now take the inner product with another, distinct eigenstate to obtain

$$\langle m| \partial_\mu H |n\rangle + \langle m| H |\partial_\mu n\rangle = \varepsilon \langle m| \partial_\mu n\rangle \quad (103)$$

since $\partial_\mu \varepsilon_n$ is a scalar and $\langle m|n\rangle = \delta_{mn} = 0$. Now we note that the second term on the LHS can be expressed as $\varepsilon_m \langle m| \partial_\mu n\rangle$ which is similar to the term on the RHS. Combining terms and simplifying, we have

$$\langle m| \partial_\mu n\rangle = \frac{\langle m| \partial_\mu H |n\rangle}{\varepsilon_n - \varepsilon_m}, \quad (104)$$

and therefore we have effectively shifted the derivative from acting on the eigenstate to acting on the Hamiltonian, which does not suffer from the random phase issue.

Recall that the Berry curvature can be expressed in terms of the imaginary part of the QGT, $\Omega_{\mu\nu}^{(n)} = -2p_{\mu\nu} = -2\text{Im}Q_{\mu\nu}^{(n)}$. We now consider expand the projection in the QGT to obtain [4]

$$\begin{aligned} Q_{\mu\nu}^{(n)} &= \langle \partial_\mu n | P_n^\perp | \partial_\nu n \rangle \\ &= \sum_{m \neq n} \langle \partial_\mu n | m \rangle \langle m | \partial_\nu n \rangle \\ &= \sum_{m \neq n} \frac{\langle n | \partial_\mu H | m \rangle \langle m | \partial_\nu H | n \rangle}{(\varepsilon_n - \varepsilon_m)^2} \end{aligned} \quad (105)$$

where in the third line we used our result for $\langle m| \partial_\mu |n\rangle$ derived above. Since we have an expression for the QGT, we can also computationally compute the real curvature $g_{\mu\nu} = \text{Re}Q_{\mu\nu}$.

Using this expression, it is clear that we do not have the issue regarding the phase of the eigenvector since they cancel out through multiplication with the complex conjugate (Hermitian-transpose). Also note that with this expression for the Berry curvature, it is becomes evident that $\sum_n \Omega_{\mu\nu}^{(n)}(\mathbf{k}) = 0$, and so $\sum_n \mathcal{C}_n = 0$ where \mathcal{C}_n is the Chern number of band n . In the simple case of a two-band model, the Berry curvature of the top band and bottom band only differ by a sign at each point in the BZ.

We do not have this issue of gauge-smoothing for the tight-binding Hamiltonian since the phase cancels out in that calculation $e^{i(\phi-\phi)} \cdot \overline{u_{0\mathbf{k}}^\alpha} u_{0\mathbf{k}}^\beta$. The issue only arises when you compare eigenstates at different points in the parameter space, or momentum in our case.

We now return to the computation of the interaction Hamiltonian. The issue boils down to computing the product of eigenvector components, $\overline{u_{0\mathbf{k}_1}^\alpha u_{0\mathbf{k}_2}^\alpha} u_{0\mathbf{k}_3}^\alpha u_{0\mathbf{k}_4}^\alpha$, which has an ambiguity of phase

$$e^{i(\phi_3 + \phi_4 - \phi_1 - \phi_2)} \cdot \overline{u_{0\mathbf{k}_1}^\alpha u_{0\mathbf{k}_2}^\beta} u_{0\mathbf{k}_3}^\alpha u_{0\mathbf{k}_4}^\beta \quad (106)$$

where we assume a phase ambiguity $e^{i\phi_j}$ associated with the eigenvector $u_{0\mathbf{k}_j}$. Luckily, this turns out to be a non-issue for our case as long as the global phase of the eigenvectors are kept track of. Different global phases amount to a unitary transformation of the Hamiltonian, which leaves the spectrum invariant.

6.3 Jordan-Wigner Transformation

Computers have a hard time dealing Grassmann numbers (fermionic statistics), and therefore it becomes useful to transform the operators. We will need to define a fermionic order (or sign convention). We define the order for creation operators as : $c_i^\dagger c_j^\dagger := c_i^\dagger c_j^\dagger$ for $i > j$, and : $c_i^\dagger c_j^\dagger := -c_j^\dagger c_i^\dagger$ for $j > i$, which implies the opposite ordering for annihilation operators, : $c_i c_j := -c_i c_j$ for $i > j$, and : $c_i c_j := c_j c_i$ for $j > i$. In summary, normal ordering requires the creation operators to the left and annihilation operators to the right. Also, the creation operators with the higher indices must be to the left, with annihilation operators with higher indices to the right. For instance, $c_1^\dagger c_0^\dagger c_0 c_1$ is normal-ordered.

We consider the action of fermion operators on our basis to see the difficulty. Naively, we may compute $c_0^\dagger |001\rangle = |101\rangle$, creating the state at site 2 (index starting from left at 0), but if we expand the state, we have $c_0^\dagger c_2^\dagger |000\rangle$ which picks up a minus sign upon normal-ordering, $c_0^\dagger |001\rangle = c_0^\dagger c_2^\dagger |000\rangle = -c_2^\dagger c_0^\dagger |000\rangle = -|101\rangle$. In general, we have to keep track of the number of states prior to the state we are creating.³⁸

In reality, we are really representing the fermion operators in a new basis, and not precisely transforming them. Generally, when performing exact diagonalization with fermions, one transforms the problem into one of spins using the **Jordan-Wigner (JW) transformation**. Spins are usually different objects to deal with as they do not exclusively behave as fermions or bosons. However, it turns out that in one-dimension, spins with $S = \frac{1}{2}$ (e.g. electrons) behave like fermions (and vice-versa). We will motivate and explore this isomorphism between fermions and $S = \frac{1}{2}$ particles in one-dimension. So we see that the only difference between hard-core bosons and fermions in one dimension is the phase we explored in the previous paragraph.

For $S = \frac{1}{2}$, we have two orthogonal spin states, $|\uparrow\rangle$ and $|\downarrow\rangle$, eigenstates of S_z . The Pauli matrices form a basis of the (real) Lie algebra $\mathfrak{su}(2)$ (unitary, Hermitian, matrices in $\mathbb{C}^{2\times 2}$), and represent observables in the space of spins. So for instance if we have a two-component spinor $|\psi\rangle$, then we could measure its spin along the x -direction by taking the trace, $\langle S_x \rangle_\psi = \text{tr}(|\psi\rangle \langle \psi| \sigma_x)$. We can also define raising and lowering operators

$$\sigma^+ = \begin{pmatrix} 0 & 1 \\ 0 & 0 \end{pmatrix}, \quad \sigma^- = \begin{pmatrix} 0 & 0 \\ 1 & 0 \end{pmatrix} \quad (107)$$

which raise and lower spin states respectively (e.g. $\sigma^+ |\downarrow\rangle = |\uparrow\rangle, \sigma^- |\uparrow\rangle = |\downarrow\rangle, \sigma^+ |\uparrow\rangle = \mathbf{0}, \sigma^- |\downarrow\rangle = \mathbf{0}$). The action of these spin raising and lowering operators appear identical to those of fermion creation and annihilation operators. In fact, the algebra is entirely replicated since $\{\sigma^+, \sigma^-\} = \mathbf{1}$,

³⁸This will be automatically kept track of by the Jordan-Wigner transformation.

$\{\sigma^+, \sigma^+\} = \{\sigma^-, \sigma^-\} = \mathbf{0}$. However, there is a problem that lies in the $\{\sigma^+, \sigma^-\}$ anti-commutation relation when we consider multiple sites. In the case of fermions, we expect the operators to anti-commute, $\{c_i^\dagger, c_j\} = \delta_{ij}$, but this fails for spins since independent spin operators commute, $[\sigma_i^+, \sigma_j^-] = 0$, instead of anti-commute ($\{\sigma_i^+, \sigma_j^-\} = 2\sigma_j^- \sigma_i^+$). Therefore in 1-dimension, $S = \frac{1}{2}$ particles are hard-core bosons, not fermions. The bridge is to construct new fermion operators out of the spin operators [15]

$$c_j^\dagger = J_j \sigma_j^+, \quad c_j = J_j \sigma_j^- \quad (108)$$

where J_j is referred to as the JW string, and is defined as [15]

$$J_j = \prod_{k=1}^{j-1} (-\sigma_k^z) \quad (109)$$

and therefore $J^2 = \mathbf{1}$. It can be readily verified that the above expressions for fermionic operators have the proper anti-commutation relations. The product symbol (\prod) denotes tensor product (\otimes), so we actually have $J_j = \bigotimes_{k=1}^{j-1} \sigma_k^z$, and further, $c_j^\dagger = (\bigotimes_{k=1}^{j-1} \sigma_k^z) \otimes \sigma_j^+ \otimes \mathbf{1} \otimes \cdots \otimes \mathbf{1}$. Note that this JW string term is non-local in that it involves the spin operator of numerous sites linked together (starting from the site 1, where 0 is the arbitrarily chosen initial site, until the site $j-1$, where j is the site of relevance). The Hamiltonians we have thus far considered (tight-binding, nearest-neighbor interaction, etc.) have solely included local terms. Therefore, after transforming the fermion operators to spin operators, the terms become non-local, and it is not clear a priori whether the Hamiltonian remains local. In fact, the locality is preserved as the non-local terms cancel. The JW transformation can be generalized to higher dimensions (two-dimensions is of relevance to us) by simply indexing the two-dimensional lattice as a chain. For higher-dimensional JW transformations, local interactions become non-local and therefore it may not be wise to transform the model if the intention is to produce a model with local (e.g. nearest-neighbor) interactions [15].

Note that the JW string J_j commutes with the Pauli operators σ_j^\pm since the string acts trivially on site j . Consider the tight-binding hopping operator, $c_i^\dagger c_j$, and its transformation to the spin basis

$$c_i^\dagger c_j = \sigma_i^+ \sigma_j^- \cdot \prod_{\min(i,j) \leq k \leq \max(i,j)-1} (-\sigma_k^z). \quad (110)$$

For ease of notation, we will define the product above as J_{ij} ($= J_{ji}$). In the special case of $i = j$, we have $c_i^\dagger c_i = \sigma_i^+ \sigma_i^- = \frac{1}{2}(\mathbf{1} + \sigma_i^z)$.

Returning to our interacting Hamiltonian, we transform each fermion operator into the spin basis using the JW transformation, and diagonalize the resulting matrix. The size of the basis is 2^{N_s} where N_s is the number of sites on the reciprocal lattice (and the real lattice). Note that since we converted the problem to momentum space, the lattice sites are the momenta.

The projected tight-binding Hamiltonian becomes

$$H_0^{\text{JW}} = \frac{1}{2} \sum_{\mathbf{k}} \varepsilon_{0\mathbf{k}} \cdot (\mathbf{1} + \sigma_k^z). \quad (111)$$

Recall that the above expression is a sum of tensor products,

$$\sigma_k^z \equiv \mathbf{1} \otimes \cdots \otimes \mathbf{1} \otimes \sigma^z \otimes \mathbf{1} \otimes \cdots \otimes \mathbf{1} \quad (112)$$

where the non-trivial term is in the k^{th} position, where $k \in [0, N_s - 1]_{\mathbb{Z}}$ is the lattice index of \mathbf{k} . The dimension of H_0^{JW} is naturally 2^{N_s} . Since we are restricting particle number, we are not computing the eigenvalues of H_0^{JW} , but will be utilizing it to find the matrix elements of our Hamiltonian. At the moment, H_0^{JW} does not restrict particle number, and allows any number of particles on the lattice. The vector space must be restricted to constrain particle number. We enforce particle number N_p by constructing a new matrix H_0 with matrix elements $\langle \{\mathbf{k}\}_{i=1}^{N_p} | H_0^{\text{JW}} | \{\tilde{\mathbf{k}}\}_{i=1}^{N_p} \rangle$.

We also transform the projected two-body interaction

$$\begin{aligned} f_{\mathbf{k}_1}^\dagger f_{\mathbf{k}_2}^\dagger f_{\mathbf{k}_3} f_{\mathbf{k}_4} &= J_{k_1} \sigma_{k_1}^+ \cdot J_{k_2} \sigma_{k_2}^+ \cdot J_{k_3} \sigma_{k_3}^- \cdot J_{k_4} \sigma_{k_4}^- \\ &= \sigma_{k_1}^+ \cdot J_{k_1} J_{k_2} \cdot \sigma_{k_2}^+ \sigma_{k_3}^- \cdot J_{k_3} J_{k_4} \cdot \sigma_{k_4}^- \\ &= \sigma_{k_1}^+ \cdot J_{k_1 k_2} \cdot \sigma_{k_2}^+ \sigma_{k_3}^- \cdot J_{k_3 k_4} \cdot \sigma_{k_4}^-, \end{aligned} \quad (113)$$

and we perform the same protocol as the tight-binding model above to compute the energies for fixed particle number, N_p . In the second line, we used that $[J_i, \sigma_i^\pm] = 0$ since J_i acts trivially on site i by definition. In the third line, we utilize our definition of J_{ij} to eliminate redundancies in the computation.

Note that we don't need to actually compute any of these matrices since their action on our basis is natural. In particular, σ_i^\pm will create/annihilate a state at site i , and our basis states are eigenstates of σ_i^z , with eigenvalue ± 1 based on whether an electron is absent/present at site i . Since the basis states are eigenstates of σ_i^z operators, they are also eigenstates of the JW strings. For each σ_i^z in the JW string, we simply apply the relevant ± 1 phase. Together, we have the actions

$$J_{ij} |\{\mathbf{k}\}_{i=1}^{N_p} \rangle = (-1)^{\#\{k \in \{\mathbf{k}\}\}} \cdot |\{\mathbf{k}\}_{i=1}^{N_p} \rangle, \quad \sigma_j^\pm |\{\mathbf{k}\}_{i=1}^{N_p} \rangle = |\{\mathbf{k}\}_{i=1}^{N_p} \pm k_j \rangle \quad (114)$$

where we restrict $\min(i, j) \leq k \leq \max(i, j) - 1$, and $\#$ denotes the cardinality, or the number of momenta k in the set of single-particle momenta of our state. In the second equation, $\pm k_j$ is pseudo for adding or removing a single-particle momentum (not vector operators). Note that adding k_j to a state that already has k_j will completely annihilate it, and similarly removing k_j from a state that does not have k_j will also completely annihilate it. Overall, particle number is conserved since there is an equal number of Pauli creation and annihilation operators. We also do not need to worry about normal ordering the fermion operators since the JW transformation takes care of that for us automatically.

7 Conclusions

The fractional Chern insulator is a fascinating phase of matter...

References

- [1] EMIL J. BERGHOLTZ and ZHAO LIU. “Topological Flat Band Models and Fractional Chern Insulators”. In: *International Journal of Modern Physics B* 27.24 (Sept. 2013), p. 1330017. DOI: <https://doi.org/10.1142/s021797921330017x>.
- [2] B Andrei Bernevig and Taylor L Hughes. *Topological insulators and topological superconductors*. Princeton: Princeton University Press, 2013. ISBN: 9780691151755.
- [3] Manfredo Perdigão Do Carmo. *Differential geometry of curves surfaces*. Mineola, New York: Dover Publications, Inc, 2018. ISBN: 9780486806990.
- [4] Ran Cheng. *Quantum Geometric Tensor (Fubini-Study Metric) in Simple Quantum System: A pedagogical Introduction*. 2013. arXiv: 1012.1337 [quant-ph].
- [5] Z. Y. Ezawa. *Quantum Hall Effects: Field theoretical approach and related topics*. World Scientific, 2000.
- [6] S. M. Girvin, A. H. MacDonald, and P. M. Platzman. “Magneto-roton theory of collective excitations in the fractional quantum Hall effect”. In: *Phys. Rev. B* 33 (4 Feb. 1986), pp. 2481–2494. DOI: 10.1103/PhysRevB.33.2481. URL: <https://link.aps.org/doi/10.1103/PhysRevB.33.2481>.
- [7] Steven M. Girvin and Kun Yang. *Modern Condensed Matter Physics*. Cambridge University press, 2019.
- [8] Douglas R. Hofstadter. “Energy levels and wave functions of Bloch electrons in rational and irrational magnetic fields”. In: *Phys. Rev. B* 14 (6 Sept. 1976), pp. 2239–2249. DOI: 10.1103/PhysRevB.14.2239. URL: <https://link.aps.org/doi/10.1103/PhysRevB.14.2239>.
- [9] Thomas S Jackson, Gunnar Möller, and Rahul Roy. “Geometric stability of topological lattice phases”. In: *Nature communications* 6.1 (Nov. 2015). DOI: <https://doi.org/10.1038/ncomms9629>.
- [10] Jainendra Jain. *Composite fermions*. Cambridge University Press, 2012.
- [11] K. v. Klitzing, G. Dorda, and M. Pepper. “New Method for High-Accuracy Determination of the Fine-Structure Constant Based on Quantized Hall Resistance”. In: *Physical Review Letters* 45.6 (Aug. 1980), pp. 494–497. DOI: <https://doi.org/10.1103/physrevlett.45.494>.
- [12] R. B. Laughlin. “Anomalous Quantum Hall Effect: An Incompressible Quantum Fluid with Fractionally Charged Excitations”. In: *Quantum Hall Effect: A Perspective* (1983), pp. 231–234. DOI: 10.1007/978-94-010-9709-3_26.
- [13] Patrick J Ledwith, Ashvin Vishwanath, and Daniel E Parker. “Vortexability: A unifying criterion for ideal fractional Chern insulators”. In: *Physical review. B./Physical review. B* 108.20 (Nov. 2023). DOI: <https://doi.org/10.1103/physrevb.108.205144>.
- [14] Biao Lian. “PHY525: Introducion to condensed matter physics”. In: *Department of Physics, Princeton University* ().
- [15] Leo Lo. “Higher-dimensional Jordan-Wigner Transformation”. In: *MIT* (May 2023). URL: <https://web.mit.edu/8.334/www/grades/projects/projects23/LoLeo.pdf>.

- [16] Titus Neupert et al. “Fractional Quantum Hall States at Zero Magnetic Field”. In: *Phys. Rev. Lett.* 106 (23 June 2011), p. 236804. DOI: 10.1103/PhysRevLett.106.236804. URL: <https://link.aps.org/doi/10.1103/PhysRevLett.106.236804>.
- [17] Rahul Roy. “Band geometry of fractional topological insulators”. In: *Physical Review B* 90.16 (Oct. 2014). DOI: <https://doi.org/10.1103/physrevb.90.165139>.
- [18] Donna Sheng et al. “Fractional quantum Hall effect in the absence of Landau levels”. In: *Nature Communications* 2.1 (July 2011). DOI: <https://doi.org/10.1038/ncomms1380>.
- [19] Steven H. Simon and Mark S. Rudner. “Contrasting lattice geometry dependent versus independent quantities: Ramifications for Berry curvature, energy gaps, and dynamics”. In: *Phys. Rev. B* 102 (16 Oct. 2020), p. 165148. DOI: 10.1103/PhysRevB.102.165148. URL: <https://link.aps.org/doi/10.1103/PhysRevB.102.165148>.
- [20] H.L. Stormer. “Two-dimensional electron correlation in high magnetic fields”. In: *Physica B: Condensed Matter* 177.1-4 (1992), pp. 401–408. DOI: 10.1016/0921-4526(92)90138-i.
- [21] Kai Sun et al. “Nearly Flatbands with Nontrivial Topology”. In: *Physical Review Letters* 106.23 (June 2011). DOI: <https://doi.org/10.1103/physrevlett.106.236803>.
- [22] David Tong. *Lectures on the Quantum Hall Effect*. 2016. arXiv: 1606.06687 [hep-th].
- [23] D. C. Tsui, H. L. Stormer, and A. C. Gossard. “Two-Dimensional Magnetotransport in the Extreme Quantum Limit”. In: *Phys. Rev. Lett.* 48 (22 May 1982), pp. 1559–1562. DOI: 10.1103/PhysRevLett.48.1559. URL: <https://link.aps.org/doi/10.1103/PhysRevLett.48.1559>.
- [24] Daniel Varjas et al. “Topological lattice models with constant Berry curvature”. In: *SciPost Physics* 12.4 (Apr. 2022). DOI: <https://doi.org/10.21468/scipostphys.12.4.118>.